Next Generation, Smart Fluid Storage Tank for Space and Terrestrial Applications

A Major Qualifying Project

Submitted to the Faculty of

Worcester Polytechnic Institute

in partial fulfillment of the requirements for the

Degree in Bachelor of Science

in

Mechanical Engineering

By

_____

Jon J. Barruetabeña

_____

Connor D. McGuirk

_____

Lily M. Ouellette

Date: 3/24/2017

Project Advisor:

_____

Dr. Jamal Seyed-Yagoobi

Abstract

The technology that will power the future of space travel will need to work smarter and last longer to drive future missions to other planets and beyond. Technology which utilizes the electrohydrodynamic (EHD) phenomena is smart and self-driven. It can be used for cooling and power purposes to achieve feats never before made possible. In 2020, NASA will be sending this next generation satellite and space technology to the International Space Station for testing. Our project explores the application of EHD conduction pumping to mix fluids non-mechanically in the absence of gravity.

Fuel and coolant storage is crucial to future long term and manned missions. If fuel or coolant contained in a storage tank is subjected to localized heat, there is risk of vapor bubbles forming in the tank. This vapor may then be released to stabilize tank pressure, but the loss of fluid is costly, and can even jeopardize the length and success of a mission. Our first-of-its-kind, EHD embedded spherical tank design actively homogenizes the temperature within and avoids vaporization of the liquid. The EHD conduction pumping mechanism provides fluid circulation via the dissociation of electrolytes when subjected to an electric field.

Our design is used for testing, which is conducted in WPI's state of the art multi-scale heat transfer laboratory. Through temperature and velocity measurements from 0 to 9,000 V, EHD mixing can be quantified for our Major Qualifying Project (MQP). The testing proves that this technology is viable and paves the way for future advancements in the field.

Acknowledgements

We would first like to thank Worcester Polytechnic Institute and the Mechanical Engineering Department for providing us with the resources and funds necessary to complete this project. The team would also like to thank Lei Yang and Michal Talmor, the PhD students in the WPI Multi-Scale Heat Transfer Laboratory for their exceptional effort and support. We would also like to thank Albert Ponsoda and Emmanuel Sionepoe for their design work preceding the project. Most of all, we would like to thank Professor Jamal Seyed-Yagoobi for advising the project and providing us with encouragement and guidance throughout the course of the project.

Contents

Table of Figures

1.0| Introduction

1.1| Overview of Electrohydrodynamics

The electrohydrodynamic (EHD) phenomena, described by the interaction between an electric field and a dielectric fluid medium, has many practical applications and is currently being researched for cutting edge space technology. This phenomenon allows for the movement of fluids without the use of traditional parts such as a mechanical pump. Instead of moving parts, an electric field induced by electrodes is used to create motion. Current research delves into the application of the EHD phenomenon in regards to pumping, mixing, and enhancement of heat transfer in dielectric fluids.

The non-mechanical functionality of the EHD phenomena makes it suitable for otherwise restricted applications, such as in environments requiring enhancement of heat transfer or mass transport as well as zero gravity environments [21]. That is why this technology shows promise in regards to the cooling of electronics in zero gravity environments such as in space. Better cooling of these electronics expands the capabilities of satellites, rockets, and the research equipment that may be onboard these vessels. Other advantages of EHD technology include, but are not limited to, smart and rapid control via alteration of the electric field, single-phase and multi-phase flow capability, and low power consumption. This technology is also lightweight and produces minimal noise [9]. However there are disadvantages as well. One disadvantage of EHD technology is a high voltage source is necessary for operation which presents both design and economic obstacles.

The properties of dielectric fluids is what allows for the EHD phenomenon to occur. The molecules within these fluids are polarized which means when an electric field is introduced the molecules will align so that the positive end of the molecule is facing the negative end of the

field and vice versa [21]. This alignment inhibits an electric flux to exist in the medium. This resistance to an electric field is a property know as permittivity, and the ratio of a materials permittivity divided by the permittivity of a vacuum is known as a dielectric constant. [8]. Dielectric fluids have very high permittivity. These fluids are used for the cooling of electronics because they have very low conductivity and therefore will not inhibit the use of the electronics [7]. An important aspect of EHD technology is that the proper working fluid be selected so that the properties of the dielectric fluid can be utilized. To achieve high efficiency, low conductivity and high mobility are necessary [21]. High-flow velocities can only be achieved with a working fluid with a high dielectric constant and low viscosity [21].

There are three types of EHD generated pumping: ion-drag, induction and conduction. Even though they share the commonality of using an electric field to move a dielectric fluid the physical process behind each one is very different. The application of these three technologies varies for this reason. However, the governing equation for the electric body force induced by the EHD phenomenon is the same for all three types and is shown below.

$$\mathbf{f}_e = \rho_e \mathbf{E} - \frac{1}{2} E^2 \nabla \varepsilon + \frac{1}{2} \nabla \left[E^2 \left(\frac{\delta \varepsilon}{\delta \rho} \right) \rho \right]$$

Where:

$\mathbf{f}_e$ is the electric body force

ρ_e is the net charge density

ρ is the mass density

E is the electric field intensity

$\mathbf{E}$ is the electric vector field

ε is the electric permittivity

This equation can be broken down into three separate forces contributing to the total electric body force. The first term is the Coulomb force, the second term is the dielectrophoretic force, and the third is the electrostrictive force. The Coulomb force requires a net charge density be present in the fluid. The dielectrophoretic force is driven by a gradient in permittivity. It cannot occur in an isothermal fluid because this fluid has no permittivity gradient as it is a function of temperature [20]. The electrostriction force has no effect on incompressible fluids because these fluids have a constant density and therefore the partial derivatives of the electric permittivity in terms of pressure would be zero [20]. This governing equation allows for a better understanding of the three types of EHD.

1.2| Ion-drag Pumping

Ion-drag pumping is a form of the EHD phenomenon in which an ion is emitted by a corona source and ejected into a dielectric fluid which contains an induced electric field. The electric field is created between the corona source and another electrode where the corona source acts as an emitter while the other electrode acts as a collector. As free charges travel along the electric field lines, the adjacent fluid is pulled into motion. The force moving the free charge is the Coulomb force from the electric body force equation.

The most research into the EHD phenomenon has been done with ion-drag. One example is research performed by Bryan and Seyed-Yagoobi, “ions were injected into the fluid within the viscous boundary layers where the electrical forces needed to overcome the highest viscous shear stresses” [21]. The pump produced velocities of approximately 33 cm/s and it was concluded that the parameters which determined the pump’s performance were fluid viscosity and electrical conductivity.

Although the most research done on the EHD phenomenon has been associated with ion-drag pumping rather than induction or conduction pumping, it is not the preferred EHD type for a number of reasons. First off, the operation of an ion-drag pump can be both inconsistent and hazardous due to the corona source. Secondly, the working fluid's electrical properties deteriorated over time when using ion drag [21]. These conditions ultimately restrict the functioning parameters of the pump and cause for a limited range of potential for the technology.

1.3| Induction Pumping

Induction pumping differs from ion-drag pumping in that charges are induced as opposed to injected into the liquid. A gradient, or discontinuity, in the electrical conductivity of the working fluid prompts the induction of these charges. The fluid is set in motion by attraction or repulsion of the charges to an AC traveling wave [21]. EHD induction pumping is most useful for the pumping of liquid films.

A first of its kind EHD induction pumping experiment was executed by Brand and Seyed-Yagoobi to investigate flow management. This experiment was conducted on the outer surface of a smooth tube where fluid flow of a thin liquid film was controlled by varying the voltage and frequency of the electric wave. Phase change was a factor present during the experiment and helped to provide insight into the enhancement of heat transfer relating to HVAC&R applications [21].

1.4| Conduction Pumping

In conduction pumping, the dissociation of molecules in a dielectric fluid results in the generation of positive and negative ions. These positive and negative ions are the charges within

the fluid which are affected by the electric field and induce a flow in the fluid surrounding them. When an electric field threshold (specific to the working fluid) is exceeded, molecules will begin to recombine at a slower rate than their dissociation rate. In other words, there is a state of non-equilibrium where ions build up faster than they can recombine back into the neutral species. Typically, an electric field on the order of 1 kV/cm is required to exceed this threshold [21]. The reaction equation for this dissociation is given as:

$$AB \leftrightarrow A^{+} + B^{-}$$

In this equation, *AB* is a neutral species with positive and negative ions A^{+} and B^{-}. The higher the threshold of the electric field, the faster the rate of dissociation and therefore the higher the charge density.

This region of non-equilibrium is called a heterocharge layer and is found in the area surrounding the electrode as shown in Figure 2. Heterocharge layers have smooth edges and a finite thickness which is dependent on the applied electric field [9]. As ions build up around the electrode, the ions of opposite polarity to that electrode are drawn to it. This creates a diffuse layer of these ions directly on top of the electrode. The movement of ions from the heterocharge layer to the diffuse layer generates movement within the fluid. A net flow in a desired direction can be obtained if proper geometry is utilized in the construction of the electrodes. If the electrodes are symmetric, an equal amount of ions will build up around the electrodes and the movement will cancel out, as in Figure 1. However, in Figure 2 a net flow is generated to the left towards the high voltage electrode because the force created by the ground electrode is canceled out due to geometry [21].

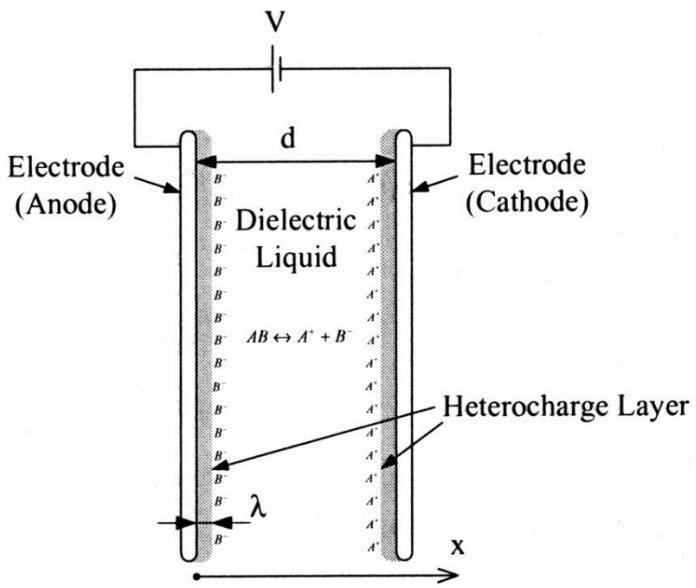

Figure 1: Dielectric Fluid between Two Electrically Charged Plates Schematic [9]

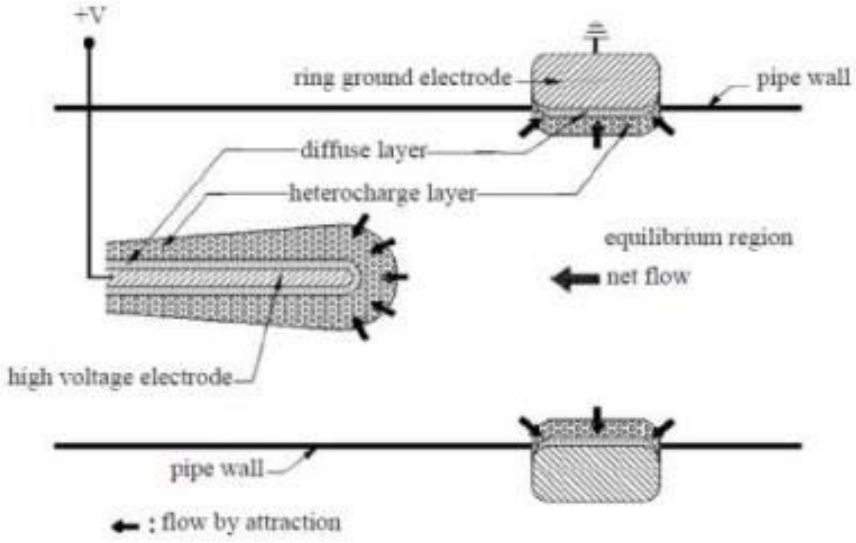

Figure 2: EHD Conduction Pumping Schematic [21]

Conduction pumping, unlike ion-drag, will not degenerate over time and does not carry any of the dangers that come from using the corona source [9] [20]. Induction pumping requires a gradient in electric conductivity, but the movement in conduction pumping is governed by the charge density of the ions in the heterocharge layers [20]. This makes conduction pumping

suitable for isothermal single phase systems, because the force driving the pumping is the Coulomb force. In an isothermal single phase system the electron body force equation can be simplified down to only relying on the Coulomb force:

$$\mathbf{f}_e = \rho_e \mathbf{E}$$

EHD conduction, while very promising, has significantly less research than the other two types of EHD technology. That being said there are many applications of EHD conduction pumping and the research that has been done shows much promise. Research into the theory behind EHD has led to the creation of numerical models to analyze the theory and make predictions. These theoretical models can then be brought to life by prototypes and experimental testing which are then compared to the models they are based off of.

1.5| Applications of EHD Conduction Pumping

1.5.1| Macro-, Meso-, and Micro-Scale EHD Conduction Pumping

Control of flow distribution by way of EHD conduction pumping has been explored and successfully demonstrated at the macro-, meso-, and micro-scale. In regards to macro-scale applications, a potential result of maldistributed liquid flow within parallel evaporators is local hotspots. If certain areas of the evaporators are hotter than others, it may cause branch lines to dry out. This occurrence will result in non-optimum performance of the heat exchanger, which can be detrimental from both an operational and economic standpoint [10]. Pertaining to the meso- and micro-scale, flow distribution control via EHD conduction pumps shows high promise in electronics cooling. At this smaller scale, EHD conduction pumping has shown success with flow distribution control for more complex configurations. Thus, EHD conduction pumps show

promise for applications such as embedded chip cooling which require thermal control of systems that are small-scale and highly branched [5] [13].

1.5.2| Single- and Two-Phase EHD Conduction Pumping

Feng and Seyed-Yagoobi have proposed a two branch mechanism that was tested using a combination of a mechanical gear pump and an EHD conduction pump [10]. Applied voltages ranged from 10 to 15 kV while mass fluxes ranged from 100 to 200 kg/m^2, which is relatable to HVAC&R applications. For a single phase (liquid) flow system, the EHD pump was shown to have a significant effect on flow distribution control. The apparatus is comparable to a heat exchanger with parallel evaporators; however, the EHD conduction pump was designed for active thermal control, as opposed to current passive methods. The level of effectiveness can be related by the power consumption and heat exchanger's redistributed heat transfer. At a measured value of approximately 1 W, electrical power consumption was negligible relative to the heat rates of existing heat exchangers found in HVAC&R applications. The experiment shows promise as heat transfer rates for such heat exchangers are often on the magnitude of kW's. A two-phase (liquid and vapor) flow system at the macro-scale was also explored, but not shown to be as effective in regards to flow distribution control. Nonetheless, significant results could be achieved by altering conditions such as applied voltage, mass flux, and vapor quality [10].

1.5.3| EHD Conduction Pumping-Driven Liquid Film Flow Boiling

Patel et al. have experimentally researched another potential solution for thermal management applications. The heat transfer method of liquid film flow boiling was studied using a surface with a metal-plated nanofiber-mat coating. As stated in the ASME Journal of Heat

Transfer article, "The nanotextured surface is formed on a copper substrate covered by an electrospun polymer nanofiber mat, which is copper-plated as a postprocess. The mat has a thickness of about 30 μm and is immersed in saturated HCFC-123 [19]." The technology was driven by EHD conduction pumping, and electrowetting of the surface was observed, analyzed, and compared to the bare surface (not containing EHD). The surface with EHD-driven flow showed a 555% enhancement in heat flux and boiling heat transfer coefficient, compared with the surface without EHD-driven flow [19]. Thus, this thermal management technique shows promise for heat-sensitive technologies, such as nuclear reactors and regenerative cooling of rockets.

1.5.4| Zero-Gravity EHD Conduction Pumping

The presence and need for removal of high heat fluxes in electronic systems has presented challenges in both terrestrial and space applications. A potential solution has been explored that involves a mechanism that uses EHD conduction pumping on the micro-scale to enhance heat transport. Yang et al. and Talmor et al. have performed experiments to prove the effectiveness of flow distribution control via EHD conduction pumping technology at the meso- and micro-scale. The experimental setups both included branches containing a "circular channel EHD conduction pump with 20 electrode pairs and a flow channel diameter of 1 mm [5][13]." Robinson et al. have expanded on the aforementioned work and have experimentally proven that their device effectively operates in both ground based and variable gravity settings [18]. The experiment involved a heat transfer loop consisting of a similar EHD conduction pump, preheater, evaporator, condenser, and reservoir. The experimental setup was installed on the Zero Gravity Corporation's modified Boeing 727 aircraft. The aircraft traced a series of parabolic curves for a number of trials as it traveled from a 1.8-g pull-in, to 20 seconds of 0-g flight, to a

1.8-g pull-out [18]. Meanwhile, a combination of instrumentation and data acquisition software was used to record data. The results acquired in the microgravity environment were coupled with the ground-based test results.

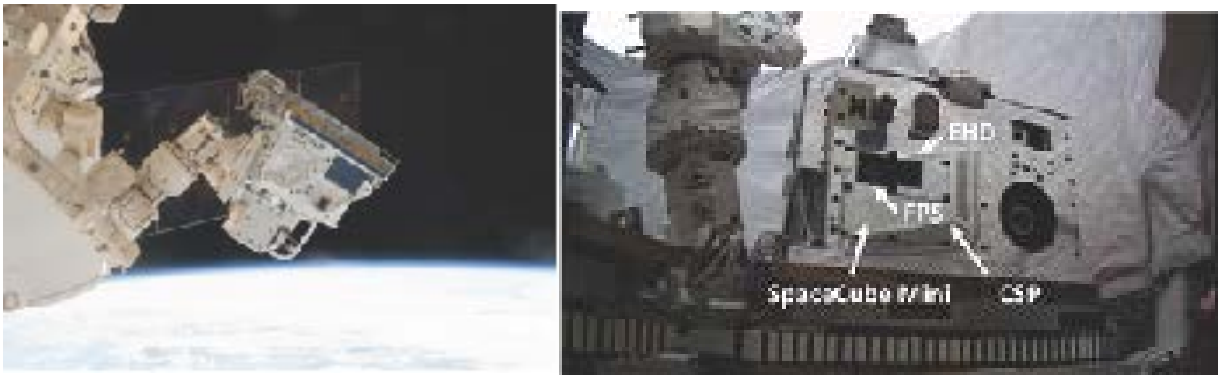

Figure 3: EHD Experimentation Equipment Onboard the International Space Station in Orbit

Pictured above is a newly installed module on the International Space Station (left) and a close-up, labeled image of a micro-scale single phase five channel EHD driven mechanism (right). Both photos were taken in space by astronauts of NASA who are using the technology to run tests. The pump was fabricated at the NASA Goddard Space Flight Center in Greenbelt, MD.

1.6| Industrial Applications of EHD

Applications of electrohydrodynamics range from pharmaceuticals and healthcare to the food industry, to electronics and space. A technique called electrospray, also known as electrohydrodynamic atomization (EHDA), has been implemented in a number of industries. Atomization deals with the molecular disintegration of a fluid medium. EHDA allows for the production and manipulation of particulate materials on the micro and nanoscale [6]. A great advantage of the generation process is the capability to develop materials with control over properties such as size and composition. Pertaining specifically to the food industry, EHDA has

been used to “spray” chocolate (for coating purposes) through a nozzle as it atomizes [3]. Use of the technology resulted in not only higher quality product, but reduced losses as well as costs. The nozzle method has also been explored in graphic arts by creating electric fields from an applied voltage, inducing fluid flow, and delivering inks to a substrate [1]. In addition, EHDA has promising potential for applications in the medical field for uses such as drug delivery and regenerative medicine.

EHD technologies are gaining increasing interest in space applications; this can be attributed greatly to the phenomena’s ability to operate in microgravity environments. NASA is currently investigating a prototype pump that utilizes EHD to provide coolant to spacecraft and their electronics. Present day arrangements have fragile mechanical parts for cooling and temperature maintenance that are subject to failure due to extreme loads and vibration experienced during launch and travel. The abandoning of these parts would reduce “size, weight and power consumption (SWaP) [15].” According to principal investigator Jeffrey Didion of the Goddard Space Flight Center, as opposed to mechanical pumps, “[EHD] uses electric fields to pump coolant through tiny ducts inside a thermal cold plate. From there, the waste heat is dumped onto a radiator and dispersed far from heat-sensitive circuitry that must operate within certain temperature ranges. Electrodes apply the voltage that pushes the coolant through the ducts [15].” These types of hardware optimization are vital to the future of space travel and exploration.

1.7| Storage Tanks for Space Applications

Space storage tanks are used to store fuel and other cryogenic fluid for spacecraft heating and cooling systems [17]. The extremely low temperature with which cryogenics deals with means any heat these tanks might be exposed to can cause vaporization of the fluid and

subsequently, a pressure increase inside the tank. To address the problem of pressure rising to the point of a catastrophic rupture of a tank, a specific design is required to eliminate the increasing pressure.

There are a few different techniques to alleviate the increase in pressure. One of the techniques used includes the venting or dumping of fluid out of the tank where volatile fluids are lost [17]. Not only is the loss of this fluid costly, it shortens the life of the cooling system or the length of a spacecraft mission. Another technique actively cools the tank contents by circulating an allocation of the contents through a system that can absorb the heat from a liquid [17]. A new technique that is being developed involves dynamic pressure control. This ventless technique mixes the fluids with or without active cooling where the tank pressurization and pressure control is conducted by interactions with forced jet mixing [17]. This technique relies on the phase change of the fluid at the vapor-liquid interface. However, because of the lack of gravity in space coupled with the very limited data availability on microgravity dynamic pressure control, systems cannot be developed for space applications using just analysis and computations alone [17].

NASA is working on a project to develop this dynamic pressure control system and has named it the Zero Boil-Off Tank (ZBOT). This tank will be tested while in Earth's gravity and in microgravity while on the International Space Station [17]. The experiment explores the effects of heat flux, fill level, mixing on thermal stratification, pressurization, and pressure control on volatile fluids. Another goal of the project is to develop a two-phase computational fluid dynamics (CFD) model for the storage tank to help next generation projects [17].

The data that will be taken during the experiment includes tank pressure, heat powers, temperature at all locations on the inside and outside of the tank, ullage position, inlet jet

temperature, tank outlet temperature, jet flow rate, gravitational acceleration data, and velocity field visualization [16]. The experiment also contains three different test categories. The first is a self-pressurization test where the heater is turned on for a desired amount of time without turning on the jet. This will determine the effect of the heater on the pressure. The next category is the mixing test. This will include setting the jet speed, then turning on the heaters, and running the heaters until either the allotted time is up or the initial pressure is regained. The last test category is the subcooled jet cooling/mixing. This focuses on specifying when and how long the jet needs to be turned on after turning on the heater. The results of this experiment have not been presently posted which implicates that NASA is still currently working on this experiment [16].

1.8| EHD Conduction for Mixing Purposes

EHD mixing is optimal for space applications as it does not have any moving parts. This is a quintessential property because it means the pump will not require human reach for maintenance, which is nearly impossible in space. EHD pumping is also ideal for space applications because it can operate in microgravity situations and it requires low power consumption. While traditional fluid mixing may depend on gravity for processes, EHD conduction mixing does not.

However, there is limited research regarding EHD mixing and much of it regards techniques unsuitable for space. A study conducted by C. Tsouris looked at using charge carriers in an electric field to mix fluid in microchannels [2]. The study was done in a “tee” geometry channel using a fluorescent dye to identify the mixing. It was found that there was a threshold in applied voltage before mixing was enhanced, however, the mixing length area where concentration fluids become uniform, shortened as the electric field applied became stronger [2].

Another study by Leslie Y. Yeo used electrohydrodynamic air thrust, also known as ionic wind, aimed at fluid in a chamber to prompt microfluidic mixing. From this research, they were able to show that this technique could be used to separate red blood cells from blood plasma for diagnostic kits [11].

However, for the implementation of cryogenic storage tanks for space application, more promise is shown in directly using EHD conduction. A numerical study conducted by Miad Yazdani and Jamal Seyed-Yagoobi analyzes the electric field, charge density, and electric body force distribution of two spherical tanks with two different electrode configurations shown in Figure 2 [22][23]. In the design of the first tank, the electrodes alternate from a slender ground electrode to a large high voltage electrode flush against the edges of the tank. This tank design is displayed in Figure 4.

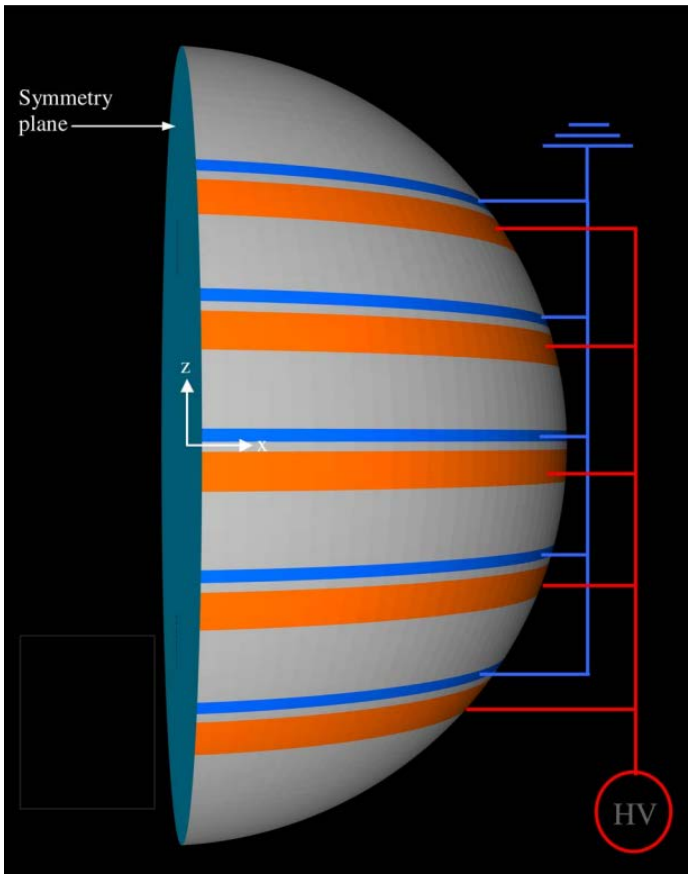

Figure 4: Diagram of Electrode Design 1 [22] [23]

The second design contains two plates of concentric rings with the high voltage electrode plate above the ground electrode plate [22][23]. The plates line up exactly so viewed from above only the high voltage electrode can be seen. This design can be seen in Figure 5 below.

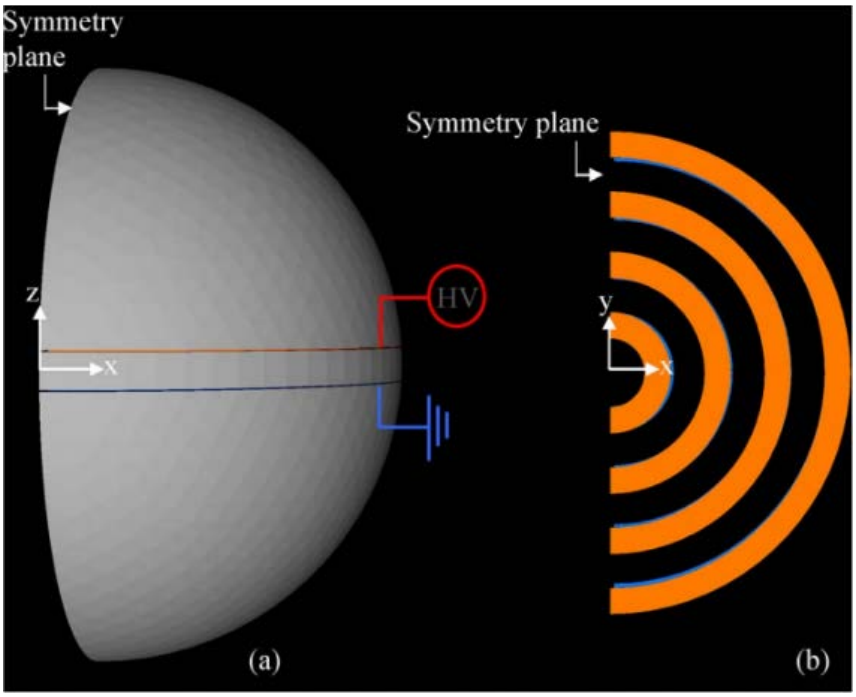

Figure 5: Diagram of Electrode Design 2 [22]

These designs were analyzed as a single phase system. The working fluid chosen was the refrigerant R-123. The study found that in the first design the electric field remained close to the reservoir inner wall and in the second design an electric field was generated within the reservoir and between/around the pair of electrodes. However, the electric body force generated for design two was only found on the middle horizontal plane. The net flow created by the first design can be described as a “donut” shape. The fluid was pushed downward along the edges of the tank and then circulated back up to the top through the middle of the tank where there was no electric field [22]. The second design had localized mixing in the center of the tank. Overall, the first design mixed the fluid better than the second design. The project discussed in depth in this report revolves around running experimental testing as a proof of concept of the validity of this numerical analysis.

2| Design & Fabrication

2.1| Design Selection

In the summer proceeding this MQP project, two French students, named Emmanuel and Albert, were working on two different designs for EHD mixing in a storage tank. This MQP began by choosing between the two designs. There were some common specifications that each design had to meet. They both needed to have a spherical tank that could contain the working fluid. They both would need connections to the high voltage supply and the common ground. Both tanks would need to have a device to heat the fluid before mixing occurs. The tanks would also need inlet and outlet valves for the fluid, and room for expansion due to pressure generated from the induced heat. Lastly, both tanks would need a method of viewing the fluid. The difference between the two tanks would be the configuration of the electrodes. Emmanuel's design, Design 1, can be seen in section view in Figure 6 below.

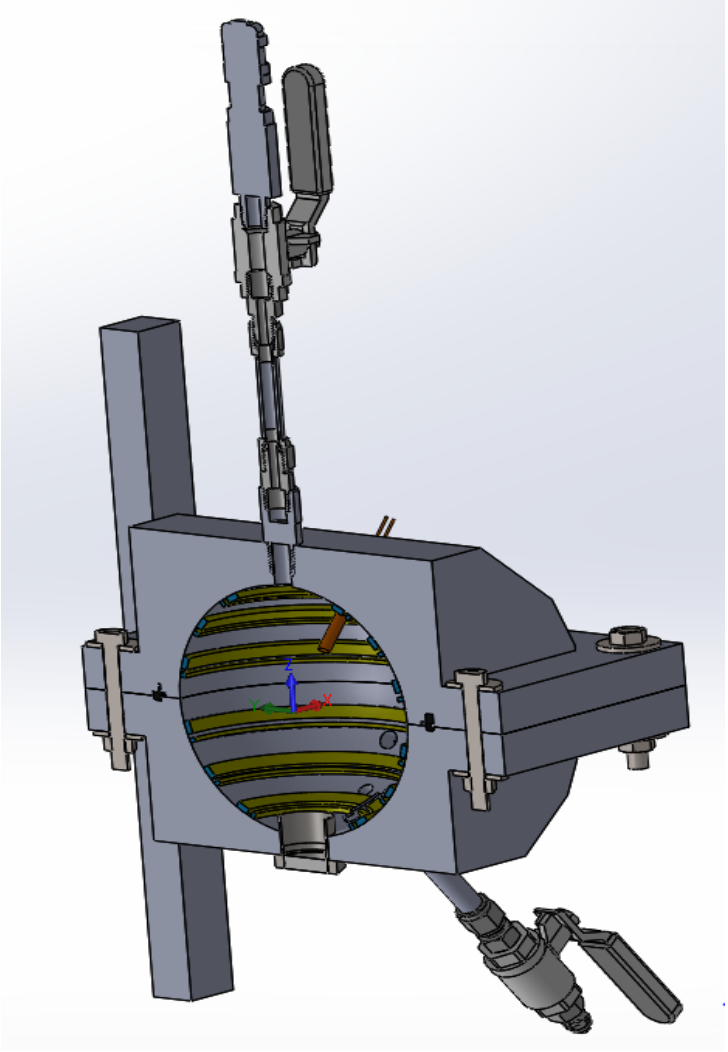

Figure 6: SolidWorks Section View of Design 1

In this design, the EHD electrodes were embedded along the wall of the tank. The second design, Design 2, was Albert's design which included the two concentric electrodes located along the center plane of the tank. A section view of this design can be seen in Figure 7 below.

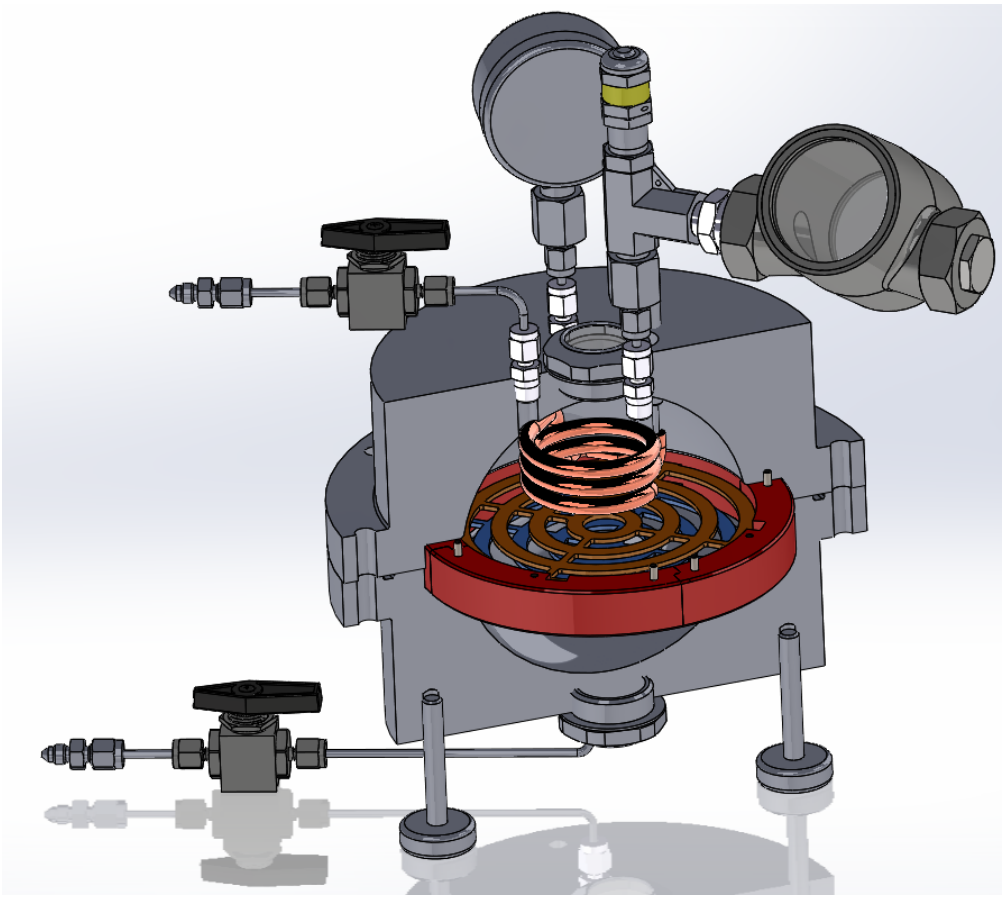

Figure 7: SolidWorks Section View of Design 2

The two designs were based off of the electrode designs found in Miad Yazdani and Jamal Seyed-Yagoobi's paper titled "Fluid Circulation within a Spherical Reservoir with EHD Conduction Pumping." In the paper, Design 1 offered the best mixing as the electrodes located on the surface of the tank broke the no-slip boundary condition rule and created mixing throughout the tank. However this design was also the most difficult to fabricate because these electrodes had to be embedded into the tank and also be flush along the walls. The Design 1 tank had a body made up of aluminum with copper as the material for the electrode. It had two insertion heaters to heat the fluid inside the tank. It also had a sight glass for visibility that also acted as an expansion valve. The design included an electrode configuration with bent copper

wire soldered together along the surface of the wall. After much discussion, it was found that this would be nearly impossible to accomplish. Another idea for the electrodes on this design included cutting grooves into the spherical walls of the tank to fit copper inside as the electrodes so they would be flush to the wall. This design also proved to be difficult as it would require extreme precision with 5-axis machining. Another problem with this design is that it was difficult to make proper insulation for the tank. The copper electrodes could not be in contact with the aluminum wall, meaning that insulation would have to divide the two materials while still leaving the electrodes flush to the wall. Overall, this design would be extremely difficult to fabricate, and a final design had not even been approved yet.

In Yazdani and Seyed-Yagoobi's paper the second design was found to not offer the high level of mixing that the first design has as the mixing was localized to the center of the tank directly around the electrodes. This second design however was much easier to fabricate. As with Design 1, the second design had a body made up of a metal, stainless steel, and the electrodes were made up of copper. There was also a sight glass that served the purpose of visibility on the bottom of the tank and another sight glass located on the top of the tank that served as room for fluid expansion. Instead of insertion heaters, it had a copper coil that served as a heat exchanger. This heater can be viewed in Figure 7. This design had insulation, a ring made up of nylon infused with fiberglass, between the two concentric electrodes and the body of the tank. Both the insulation ring and electrodes were very feasible to manufacture.

Due to the fact that creating electrodes of the first design was very difficult, the second design with the concentric electrodes along the center of the tank was chosen. This design was chosen because the main goal of the project was to prove the concept of EHD mixing, so the design that would most certainly be able to be fabricated was necessary. If the first design was

chosen, there was a possibility that the electrodes would not be able to be made at all, which would be a failure to the main goal of the project.

2.2| Fluid Selection

Two different types of fluids could have been used for this project. The two choices were a refrigerant or a type of vegetable oil. The refrigerant would be the type of fluid that would be used for space cooling applications, but with a refrigerant, there can be no leaking. Vegetable oil is more safe to work with, is inexpensive, and there would be little to no consequences if leaking occurs. Due to the extreme design and safety constraints of refrigerant, a vegetable oil known as corn oil was chosen to be used for EHD mixing. The corn oil that was chosen was Price Chopper brand, pure corn oil.

2.3| Design Modifications

After further evaluation of the design, it was necessary to make some design changes. The material of the tank was changed to a clear plastic so that it would be possible to view the mixing within the tank. Plastic is also more insulated than stainless steel, which poses a much smaller risk of creating a charge on the body of the tank. Since plastic is prone to cracking, the material of all of the screws and other fasteners was changed from stainless steel to brass. Brass is softer than steel and reduces the risk of cracking the tank. The electrode design was then changed. Originally, asymmetry was accomplished by offsetting the electrodes so that the concentric rings were in opposite places, but this would not work because it was necessary to be able to pass measurement devices between the rings. This original design created by Albert is

pictured below. The gold color represents the high voltage electrode and the blue represents the ground electrode.

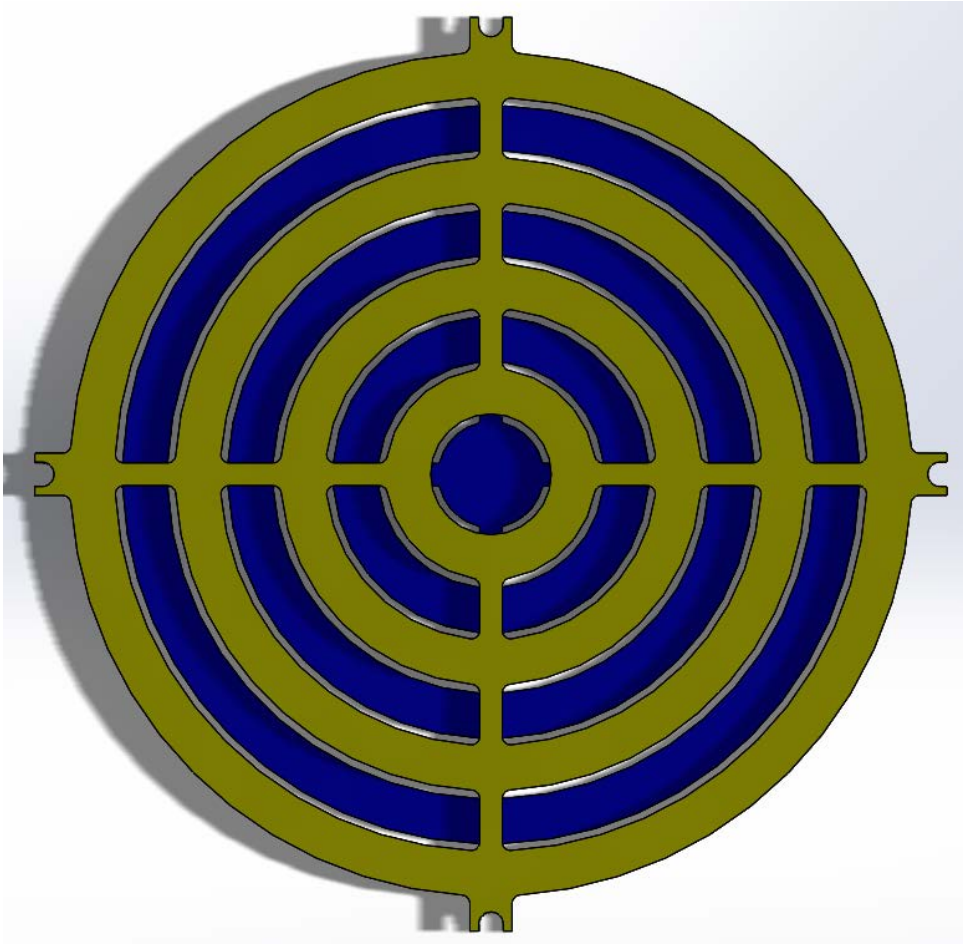

Figure 8: Top View of electrode configuration 1

To fix this, the high voltage electrode was changed to be half the size of the ground electrode to create the asymmetry. The center of each concentric ring for both electrodes was placed in the same location. With a gap in the center of each electrode, the measurement devices were able to pass through. The thickness of each electrode remained as 2 mm, but the distance between the inner surfaces of each electrode was changed from 6 mm, to 3 mm. This design can

be seen in the Figure 9. The gold color displays the high voltage electrode, and the blue displays the ground electrode.

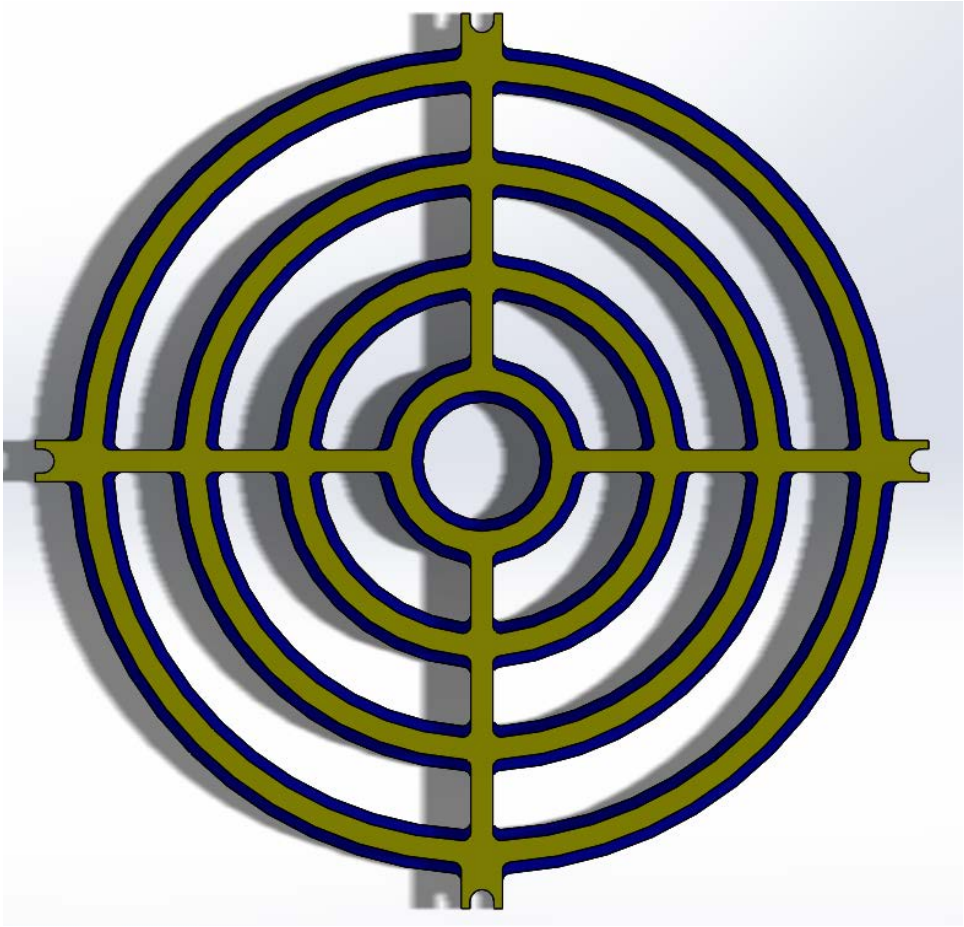

Figure 9: Top View of Electrode Configuration 2

Another design was created where the center of the rings was slightly offset. The thickness of each ring remained the same, but the gap between each ring was adjusted so that there was a 1 mm horizontal gap between the closest edge of each electrode. The gap between the inner surfaces of each electrode remained at 3 mm. This design change allowed for a larger mixing effect than the previous electrode configuration. This is the configuration used for the final assembly of the electrodes. This configuration can be seen in Figure 10. The high voltage electrode is again gold and the ground electrode is blue.

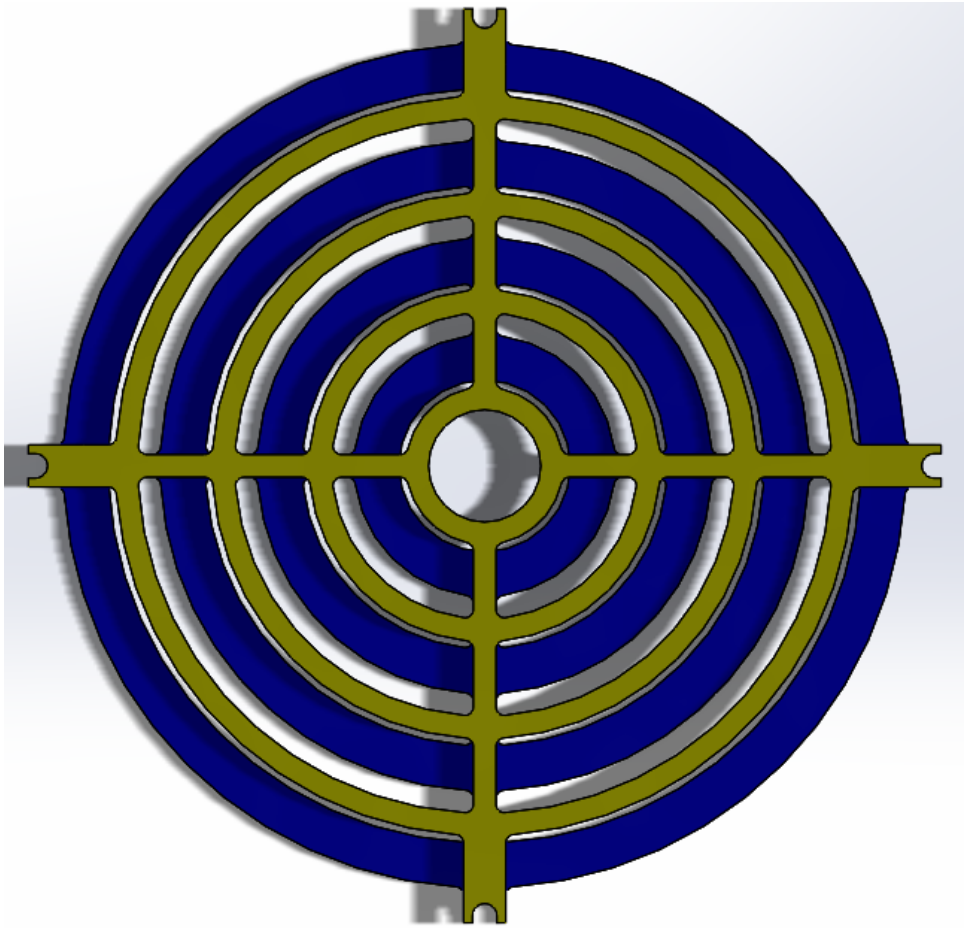

Figure 10: Top View of Electrode Configuration 3

These electrodes are attached to wires that run out of the top of the tank to the high voltage supply box and to the common ground.

The heating device was changed from a copper coil that served as a heat exchanger to a cartridge immersion heater. The heating device was changed because the copper coil took up too much space within the tank to be able to have measurement devices. This heater has a maximum output voltage of 240 V and a maximum output power of 400 W, allowing it to heat the tank to well above the desired value. A sight glass was added into the side of the tank as well, in case the visibility of the plastic was not as transparent as expected. The final SolidWorks design is pictured in Figure 11 below.

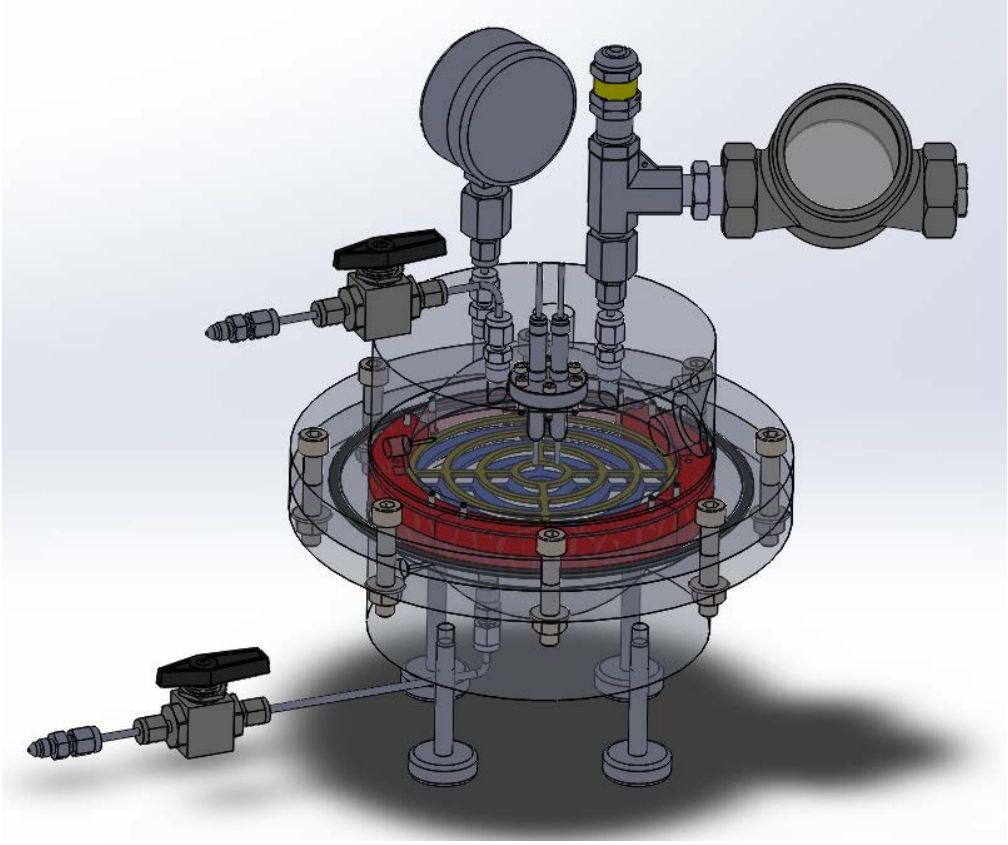

Figure 11: Final Tank Assembly

2.4| Measurement Devices

The measurement devices used to gather data during experimentation included two pitot tubes, two thermocouples, and a RTD. Pitot tubes work by measuring pressure difference, which then allows the user to calculate velocity using the following equation:

$$V = \sqrt{\frac{P_t - P_s}{\frac{1}{2}\rho}}$$

Where:

V is the velocity of the fluid

P_t is the total pressure

P_s is the static pressure

ρ is the density of the fluid

The measured pressure difference is between static pressure and stagnation, or total pressure. One end of the Pitot tube was inserted into the tank. The other end of the Pitot tube connected to a t-connector and further to tubing that made the connections with the pressure transducer. The thermocouples provided an overall temperature reading for the top and bottom halves of the tank. The pitot tubes and thermocouples were inserted into the sides of the tank using compression fittings; one of each device into the two halves of the tank. The RTD was inserted into the center of the top of the tank and is capable of sliding from the top to the bottom of the tank, through the electrodes' center holes. Thus, the RTD measures continuous temperature readings as it moves through the tank allowing it to develop a temperature profile.

2.5| Fabrication

Initially, fabrication for the tank was going to be done off campus. A number of different custom plastics companies were contacted. Those who were capable of manufacturing the tank design generated quotes that were too far over budget. Instead, the rapid prototyping department at WPI was used for tank fabrication. An information session held about 3D printing helped determine that by using WPI's Objet260 Connex Rapid Prototype machine and the material Veroclear, a suitable tank would be able to be produced to fulfill our purposes. The tank was printed with all of its features including many holes for fittings and screws. However, as threads do not print well, the threads were manually tapped in Washburn Shops at WPI. A test block of

the Veroclear material was ordered with two holes to practice tapping on for the purpose of avoiding making any mistakes while threading the holes for the tank.

Another important aspect of the project pertaining to fabrication was the electrodes. Albert had been in contact with a hydro cutting company, HydroCutter Inc, that offered to hydro cut the electrode design for free. The necessary copper for the ground and high voltage electrodes was provided to them along with the design schematics, but the product received from the company was scaled down too small. To address this problem, copper stock was ordered and the electrodes were machined using the MiniMills in Washburn Shops. Since the MiniMills are CNC machines, they require a NC code to be able to run the program. To generate this code, a solid model was imported into a computer-aided manufacturing (CAM) program, ESPRIT. In ESPRIT, a toolpath and different operations to machine the electrodes were developed. The program was then able to generate the NC code using its post processor. The next step was to fixture the copper stock into the MiniMill in a way that it could be successfully machined. Due to the small thickness of the copper, it had to be fixtured it to a thicker piece of aluminum using a special type of wax called Mitee Grip. The wax paper was placed between the copper and aluminum on a hot plate. The hot plate then heats all the materials until the wax melts. At this point, everything was removed from the hot plate. Once the wax cools, the copper and aluminum are attached with great strength, allowing the copper to be machined. In the MiniMill, the aluminum was fixtured to the table using machine straps. After the stock and tools are probed, the copper was machined using a 1/8" end mill. When the machining was finished, it was necessary to reheat the aluminum and copper to melt the wax and detach the copper from the aluminum. An image of the machined copper being removed on a hot plate is pictured below.

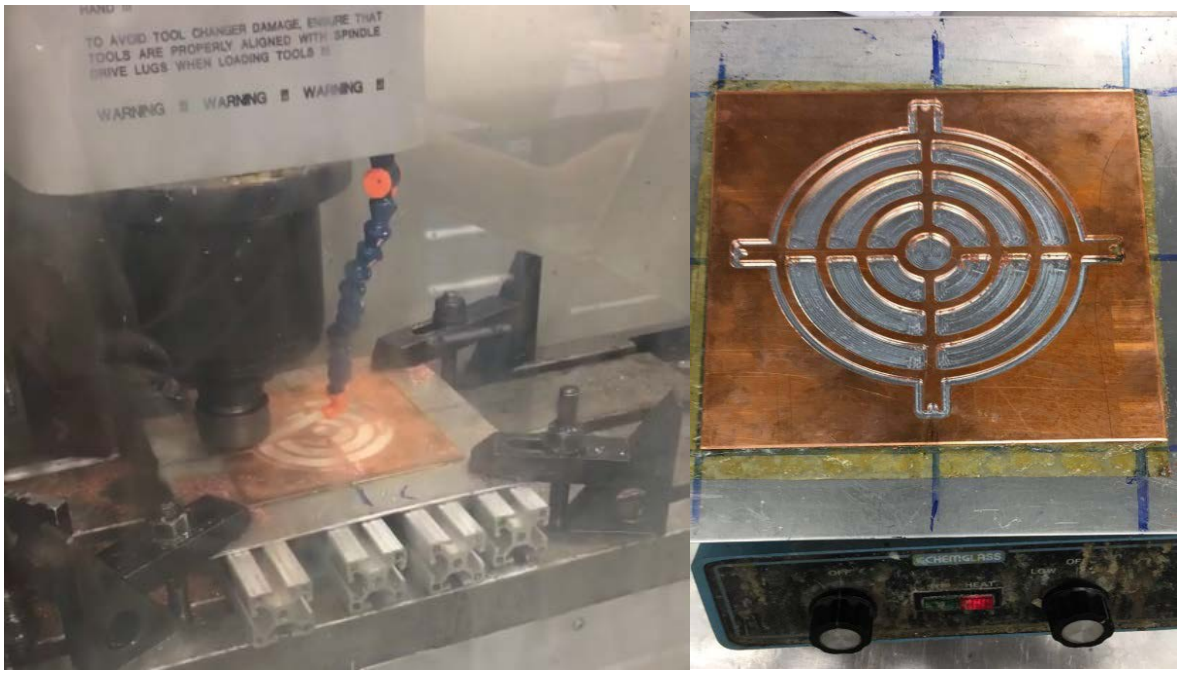

Figure 12: Machining of Top Electrode (left) Heating of Mitee Grip for Part Removal (right)

The copper was then deburred and put into a mass finisher to create smoother edges. The finished copper electrodes are pictured in Figure 13.

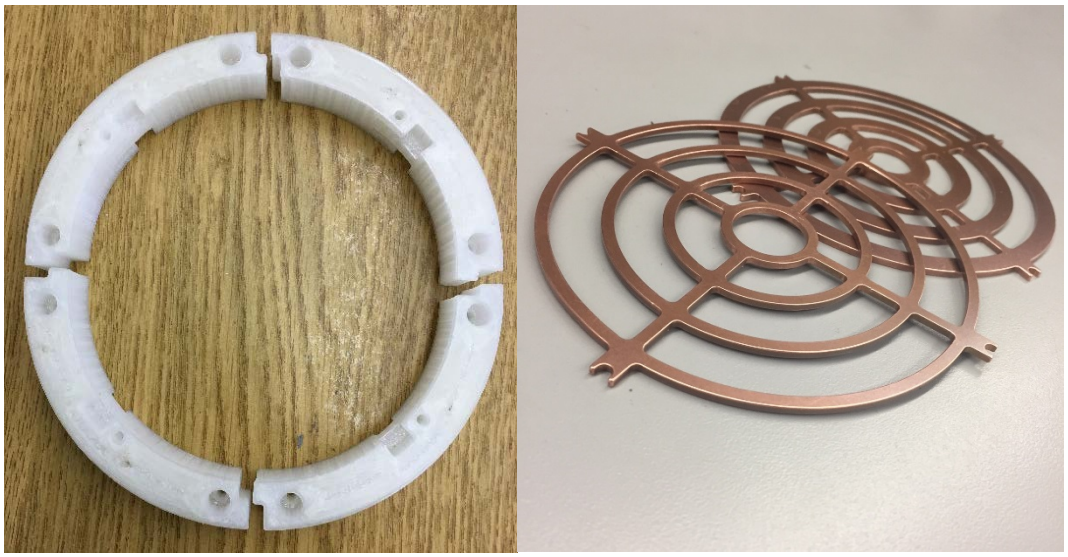

Figure 13: 3D printed insulation ring (left) Electrodes after being cleaned and removed from the mass finisher (right)

The electrodes were held in place inside the tank by a four-piece insulating ring. This ring has also been 3D printed by the WPI rapid prototyping department using the Mark 2 rapid prototype machine. This machine is specifically used for creating the nylon infused with fiberglass material. These insulate rings can be seen in Figure 13.

To attach the electrodes to the high voltage supply and common ground, a 20 kV rated wire was soldered onto the electrodes. Due to the fact that a soldering iron could not heat up the electrodes enough to connect with the solder, a blow torch was used. The blow torch was able to easily heat the copper electrodes enough to attach the wire with tin solder. This connection was then tested using a multimeter. Originally the wires were to be attached to a high voltage feedthrough, but due to the difficulty of installing this and the low voltage rating, the wires were fed out of separate holes and directly attached to their connections to the high voltage supply and common ground. Removing the high voltage feedthrough caused the layout of the top of the tank to change. The high voltage feedthrough holes were filled in with epoxy. The pressure gage hole was used as the outlet for the wire from the high voltage electrode. The expansion vessel hole was replaced with the outlet for the ground electrode. The inlet valve was extended to include a sight glass which served as the expansion vessel. The sight glass made it possible to see how much the fluid expanded. The pressure gage was removed from the entire setup as it was not needed because differential pressure transducers were already included in the setup.

Many compression fittings were necessary for the fabrication of the tank. They are needed because they allow devices such as the pitot tubes and thermocouples to be inserted into the tank without the fluid leaking out of it. Due to the way the compression fittings are made, relative to the measurement device diameters, it was necessary to drill a slightly larger hole in the fittings for the pitot tubes and thermocouples. These holes were drilled using the manual drill press in

WPI's Washburn Shops. The RTD fitting did not need to be drilled because it was purchased to fit a fraction of a size larger in diameter to allow the device to slide freely through the fitting, while maintaining somewhat of a seal. This loose fitting is allowed due to the fact that the probe moves vertically from the top of the tank and the working fluid is corn oil can leak safely.

To make the tank transparent, the inside of the tank was polished using sandpaper. The process started with the use 220 grit sandpaper. After the 220 grit sandpaper generated a smooth feel, the 320 grit sandpaper was used, and finally the sanding was finished using 400 grit sandpaper. This sanding changed the rough inside of the tank into a very smooth surface. When liquid is put into the tank, the top becomes completely transparent, allowing the electrodes to be visible. After all of the necessary adjustments were made to the parts, the tank was assembled. Below is an image of the tank, fabricated and assembled for experimentation.

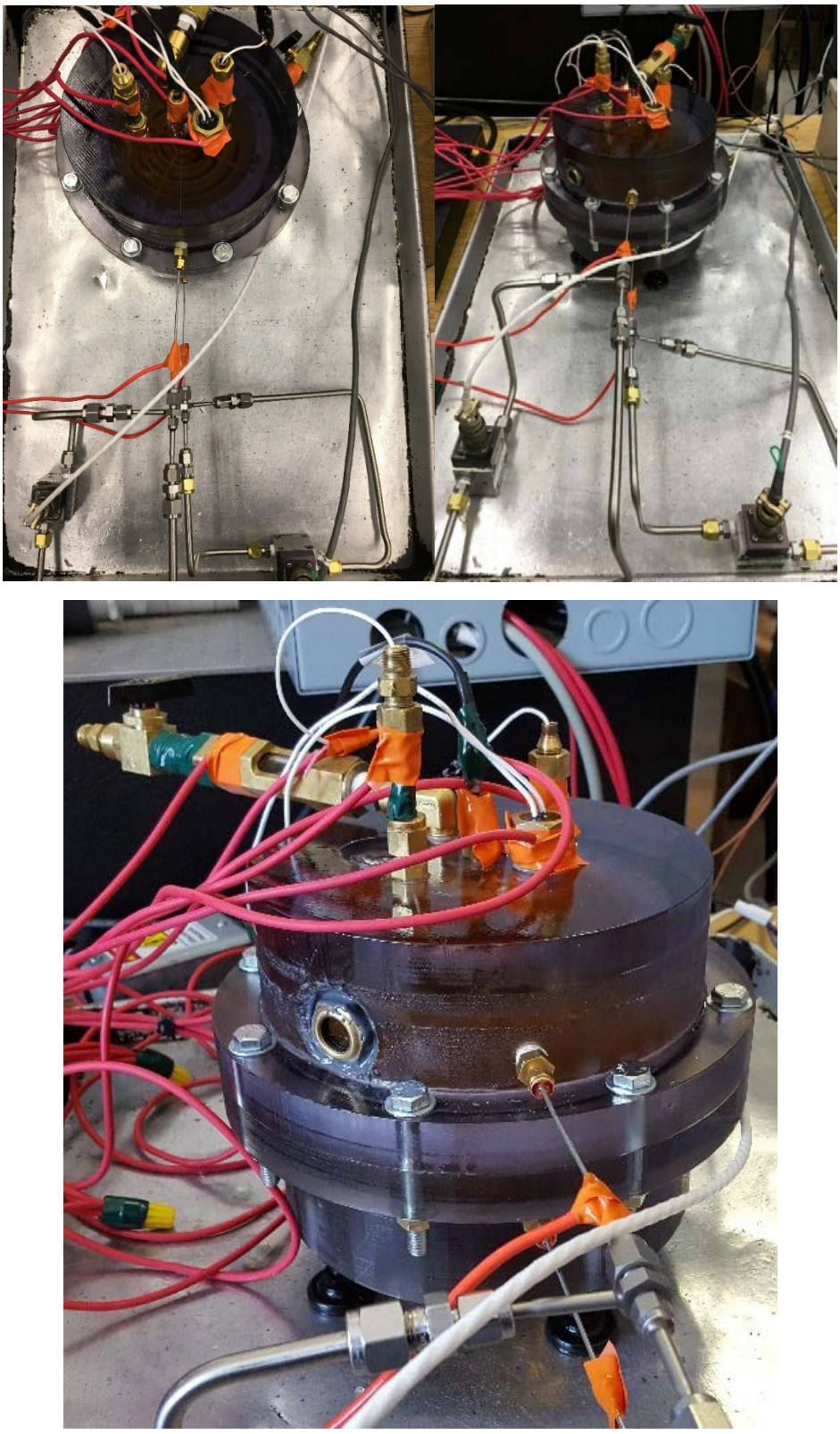

Figure 9: Assembled EHD Storage Tank ready for Experimentation

3| Methodology

To restate, the goal of experimentation was to achieve measurable proof of non-mechanically induced mixing, by the means of the EHD phenomena. The analyzed data includes voltage, temperature, pressure, and velocity readings. More specifically, this data was monitored to look for variations in internal pressure and temperature over time as evidence of mixing. To ensure this data could be properly collected, a data acquisition program was created, equipment was calibrated, the permittivity and resistivity of the oil was measured, and the electrodes were tested before the experiment itself was run.

3.1| Data Acquisition

To monitor and record data during experimentation, a data acquisition program was written using the National Instruments software LabVIEW. Data acquisition software, coupled with the proper instrumentation, is necessary when running an experiment as it allows the user to simultaneously control multiple outputs to the system, as well as read in and write out information from the system through input channels. Pertaining to the experiments, the voltage for both the EHD electrodes and heater needed be controlled, and the returning voltage and current needed to be monitored and recorded. Temperature data and velocity data were also monitored and recorded using measurement devices contained within the tank.

To connect each of the various measurement devices to the computer, two data acquisition boxes were required. One box contained the channels for voltage outputs, voltage inputs, and current inputs. This box was specifically used for the EHD high voltage supply, heater voltage supply, and the pitot tubes. The other box contained the channels for the

temperature inputs. This box was specifically used for the RTD and the thermocouples. From the computer, these channels could be controlled using the LabVIEW program which was made up of a block diagram and a front panel. The block diagram was responsible for the inner workings of the program. It contained features such as the DAQ assistants, conversion equations, a write to file module, and a timing module. An important feature of the program was the VI shutdown. The VI shutdown feature would automatically stop the program from running if the predetermined EHD current limit was exceeded. The front panel of the program served to start/stop the program, press to record data to a file path, and to control voltage outputs, current limit, and calibration values. The front panel also contained a waveform chart for each of the parameters and indicators for elapsed time and whether the current limit was being exceeded or not. Visuals of the block diagram and front panel can be found in Appendix A and Appendix B.

3.2| Calibration

In order to generate accurate readings, it was vital to ensure all equipment was calibrated properly. LabVIEW is equipped with built in calibration for RTDs and thermocouples. This feature was utilized for calibrating this equipment in the experiment. Therefore, the only pieces of equipment that required calibrating were the two differential pressure transducers to be used with the two pitot tubes. The pressure transducers were calibrated using an air supply connected to a pin valve and a manometer. The positive end of the transducer was connected to the air supply and the negative end was exposed to open air. The air supply was also connected to the manometer using a t-connector. Voltage readings from the pressure transducer were recorded using a National Instruments software, NI Max, on the computer. The corresponding pressure values were taken from the manometer. A calibration curve was calculated by graphing pressure

with respects to voltage and using the line of best fit feature on Microsoft Excel. This curve can be found in Appendix C. Six observations for voltage and pressure were used to generate the calibration curve. The equation for the pressure transducer used for the top Pitot tube was found to be:

$$P_{top} = 97.99 * V_{top} - 495.35$$

The equation for the pressure transducer used for Pitot tube located on the bottom of the tank was found to be:

$$P_{bot} = 54.74 * V_{bot} + 220.76$$

The regression generated showed strong correlation with an R^2 value of 0.9807 and 0.9964 for the top and bottom pitot tubes, respectively. The slope and intercept values of equation generated for the line of best fit were entered into the LabVIEW program.

3.3| Voltage Supplies

Two voltage supply sources were used to complete this experiment. One voltage supply was used with the EHD electrodes and the other was used for the cartridge insertion heater. For the electrodes, a high voltage supply with a maximum output of 30 kV and 3 mA was used. The voltage supply used for the heater had a maximum output of 120 V and 6 A. Both voltage supply boxes are pictured below.

Figure 14: EHD High Voltage Supply Box

Figure 15: Heater Voltage Supply Box

Both supplies were controlled from the LabVIEW program. The way LabVIEW does this is by sending out a small amount of voltage that corresponds to a much higher voltage to be sent out by the high voltage supply box. The ratio of this voltage is specific to the voltage supply. For the EHD high voltage supply box this ratio is 1:10 and for the heater's voltage supply box this ratio is 1:10. The way that this works in LabVIEW is an input of 1 to the voltage for EHD high voltage supply in the program would correspond to 3 kV. An input of 2 would correspond 6 kV. These ratios were worked into the LabVIEW program so the voltage could be easily controlled and monitored from the front panel of the LabVIEW program. This was done by dividing the input value of the actual value in LabVIEW to match the ratio of either voltage supply, and then multiplying the ratio received from the voltage supply to read the actual value of the voltage.

To safely use the equipment, every conductive material that would be in contact with the inside of the tank was connected to a common ground located on the back of the high voltage supply. A multimeter was used to test every connection to ensure all of these components were

grounded. This multimeter was also used to ensure the EHD electrodes were connected to the high voltage supply and ground respectively and to ensure that there was nothing connecting the electrodes to each other.

When trying to run the experiment, initially there were issues supplying high voltage to the electrodes. If the voltage was set to 5 kV, sparks could be heard coming from the system and the LabVIEW program would crash. It was found that these sparks were coming from a connecting piece that connected a RG-8/U coaxial cable to the 20 kV rated wired connected to the high voltage electrode. To fix this problem the connecting piece was removed and the 20 kV wire was connected directly to a RG-9/U cable.

3.4| Testing the Working Fluid

For the experiment, the permittivity and resistivity of both filtered and unfiltered corn oil was tested to determine the best state the corn oil should be in to run the experiment. The filtered oil was passed through a two micron filter to remove impurities. Then the permittivity and resistivity of the filtered oil, as well as unfiltered oil, were calculated from resistance and capacitance measured using a test cell seen in Figure 16.

Figure 16: Test Cell for Working Fluid Measurements

The test cell consisted of an outer and an inner cylinder made out of steel attached to a teflon piece. The test cell was filled with oil to the top of the inner cylinder and then a capacitance meter was attached to both the inner and outer cylinder of the test cell to find the capacitance. Next, a multimeter was attached to the inner and outer cylinder of the test cell to measure the resistance. The equations used to calculate the permittivity and the equation used to calculate resistivity can be found below.

$$A_t = \frac{2\pi L_1 l}{\ln\left(\frac{r_o}{r_i}\right)}$$

Where:

A_t is the axial area at the midpoint of the annulus of the test cell

L_1 is the height of the test cell

l is the length of the gap between the outer and inner cylinders of the test cell

r_o is the inside radius of the outer cylinder

r_i is the outside radius of the inner cylinder

For these calculations, the length of the gap between the outer cylinder and inner cylinder divided by the axial area at the midpoint of the annulus of the test cell was a constant value that was calculated to be 0.19 for the test cell used. This value was then multiplied by both the capacitance and resistance measured to get the permittivity and resistivity respectively. The permittivity and resistivity for unfiltered oil was calculated to be 33.4 pF/m and 28.5 GΩ/m respectively. The permittivity and resistivity for filtered oil was calculated to be 34.4 pF/m and 15.2 GΩ/m respectively.

$$e = C\left(\frac{l}{A_t}\right)$$

$$\tau = R\left(\frac{A_t}{l}\right)$$

Where:

l is the length of the gap between the outer and inner cylinders of the test cell

A_t is the axial area at the midpoint of the annulus of the test cell

e is the permittivity of the oil

C is the capacitance of the oil

τ is the resistivity of the oil

R is the resistance of the oil

The tank was first filled with filtered oil and then was checked for leaks. Adjustments were made to the fittings to prevent leaking coming from the thermocouple fittings as well as the outlet valve fitting. Air was bled out of the pitot tubes by leaving one end open and waiting for oil to leak through. Then pipettes were used to fill the tubing connecting the pitot tubes to the pressure transducers. The experiment was initially run with filtered corn oil; however, after issues with the testing, this oil was switched out for unfiltered oil in an attempt to increase the efficiency of the experiment by increasing the electrolytes in the working fluid.

3.5| Electrode Testing

It was imperative that the electrodes in the setup be smooth and contain no sharp edges. Any sharp edges in the electrodes could cause EHD ion drag to occur instead of EHD conduction. Ion drag can degrade the electrical properties of the dielectric fluid over time and thus would have been unfavorable to the testing. To confirm that there was no chance of ion drag happening during the experiment a test was done with the electrodes. During the test a voltage was applied across the electrodes while there was no liquid in the tank. Voltage was applied from 100 V to 600 V at an increment of 100 V. If the electrodes had contained sharp edges, the ions

would have been escaping from the electrodes and there would have been a buzzing sound heard coming from the set up. As no noise was heard while running the test, it was concluded that the electrodes were smooth enough to use in the experiment.

3.6| Experimentation

Data was collected for both velocity and temperature during this experiment. For the velocity data, the pitot tube on the top half of the tank was facing the high voltage electrode 30 mm horizontally into the tank. The pitot tube on the bottom half of the tank was facing the ground electrode, also 30 mm horizontally into the tank. Data was collected in one trial without any heat being added from the heater. The voltage used to run this experiment was 9,000 V.

The temperature data was collected for the experiment in four separate trials. Half of the trials were conducted while running EHD conduction, while the other half of the trials were conducted without EHD as an experimental control. For every experiment the tank was first heated by supplying 72 V to the cartridge heater for five minutes. This produced a heat flux density of 433.72 W/m^2. The calculations for this chosen voltage and time period can be found in Appendix D. The heater was then turned off and for experiments run without EHD temperature data was recorded for 3 hours after turning off the heating element. For trials run with EHD, the high voltage electrode was supplied 9000 V and left to run for over an hour, until the temperature readings reached equilibrium. For all four trials, the two thermocouples were kept in the same position. Each thermocouple was located approximately one centimeter away from the vertical center line of the tank and 30 mm either above or below the center horizontal plane of the tank. For the first two trials the RTD was positioned approximately 12 mm from the top surface of the

tank and along the vertical centerline. For the fifth and sixth test the RTD was located in the absolute center of the tank between the electrodes with is 60 mm inside the tank.

4| Results & Discussion

This MQP gathered results for two different types of measurements. The first set of data that was gathered was the velocity data, and the second set was the temperature data.

4.1| Velocity Measurements

After running the EHD high voltage supply at 9,000 V without the heater turned on, it was proven very difficult to find any accurate velocity measurements. A simulation of the setup running with this applied voltage showed that a velocity of 0.5 m/s would be generated right above and below the center of the electrodes. When testing for this, multiple problems arose. The differential pressure transducers constantly were producing negative pressures, even after calibration. To address this issue, the y-intercept value for the calibration curve was adjusted so that the pressure readings were at zero. Once the EHD high voltage was turned on, the pressure readings and the velocity readings made no significant changes to indicate that the electrodes were even working. Even if the measured velocity rose, it never came close to reaching the simulated velocity of 0.5 m/s. Also, when the EHD high voltage was shut off, the velocity would in theory immediately regress to where it started before the voltage was applied. This never happened when the EHD high voltage was shut off, as it never regressed at all. Adjustments were made to the directions that the pitot tubes were facing, and still none of the pressure readings or velocity readings indicated any presence of EHD.

Due to the lack of results from the pitot tubes, it appeared that the L-shaped pitot tubes used were not a sufficient device to measure the velocity of corn oil from EHD mixing in a spherical tank. There are a few different reasons why the pitot tubes failed to produce results. One problem could be that the diameter of the holes on the pitot tubes used for measurement were too for small for the corn oil. The size of these holes were 355.6 microns. To be able to measure corn oil, the size of the holes can be a minimum of 300-400 microns. Although the pitot tubes used met this requirement, the holes were still very close to minimum requirements. Another possible issue with the pitot tubes could be that there was air within the tubing connecting to the differential pressure transducers. Since air is a compressible fluid, it would affect the pressure measured from just corn oil. Even though the pitot tubes were bled to drip oil before they were attached to the tubing, and the tubing was filled with corn oil from a pipet until leaking before attachment, air could have been present during reattachment of the tubing to the pitot tubes.

The last issue that could have arose is the angle that the pitot tubes can measure could have been too small. The pitot tubes have trouble measuring accurately when the flow is not parallel to the head of the pitot tube. If the flow is greater than 5^{o} from being parallel to the head of the pitot tube, then the reading begins to become inaccurate. If the flow is 30^{o} from being parallel to the head of the pitot tube, the readings are inaccurate by a factor of 2% or more. Judging by the inaccuracy of the measurements from the pitot tubes when running the experiment, it appears that the flow could have been much greater than 30^{o} from being parallel to the head of the pitot tube. The characteristic of the flow generated from the concentric electrodes moves in a spiraling motion as it moves towards the surface of the tank. The motion at the center of the electrodes is the closest to moving parallel to the electrodes, as in the simulation it appears

the flow is moving vertically at the center. The pitot tubes were located in the center of the tank facing the electrodes, but due to the nature of the flow around the concentric rings, it is highly possible that the flow was more than the maximum angle from being parallel to the head of the pitot tube needed to measure accurate velocity readings. Since the pitot tubes failed to produce results proving the concept of EHD mixing, the proof of EHD relies heavily on the temperature readings in the experiment.

4.2| Temperature Measurements

4.2.1| Trends in Tank Cooling

The temperature measurement data displayed in this section is broken up based on the test run. Figure 17 shows the test run without EHD when the RTD was positioned in the center of the tank and Figure 18 shows the test run with EHD while the RTD was positioned in the center of the tank. For these tests, the thermocouples were in their constant spots of 20 mm from the center of the tank on the top and bottom while the RTD was placed between them in the center of the tank. In Figure 17, the process of heating up the tank for five minutes and letting it settle back to an equilibrium point naturally can be seen. It took about 19,000 seconds, or about 5 hours and 15 minutes, for the tank to cool back down to its starting temperature. The long amount of time it takes for the tank to reach its starting point is actually attributed to the insulative nature of the tank and is also dependent on the ambient temperature in the room. As you can see, the temperatures from the top and bottom of the tank did not start out equal and are almost 1 ^{o}C different from each other at almost 12,000 seconds, or 3 hours and 20 minutes. The heater caused the biggest temperature rise for the top thermocouple which makes sense as it was the closest of the three devices to the heater during this trial. Overall, the temperature of the top thermocouple

rose about 5 ºC. Even after the heater was off, the temperature for the top thermocouple continued to rise. The temperature increase for the RTD was smaller than the top thermocouple because it was not as close to the heater. The temperature rose about 2 ºC. The bottom thermocouple's temperature did not rise at all while the heater was running. The temperature seemed to have decreased by a small amount. This was most likely due to the temperature of the bottom of the tank being unsteady when the experiment was started. After about 5,000 seconds, or about 1 hour and 20 minutes, the temperature of the bottom thermocouple began to rise and match the temperatures at the middle and top of the tank. There was a sudden drop in the data at about 25,000 seconds. It is unclear what would have caused this decline but the most likely answer is the temperature in the room also dropped suddenly around that time.

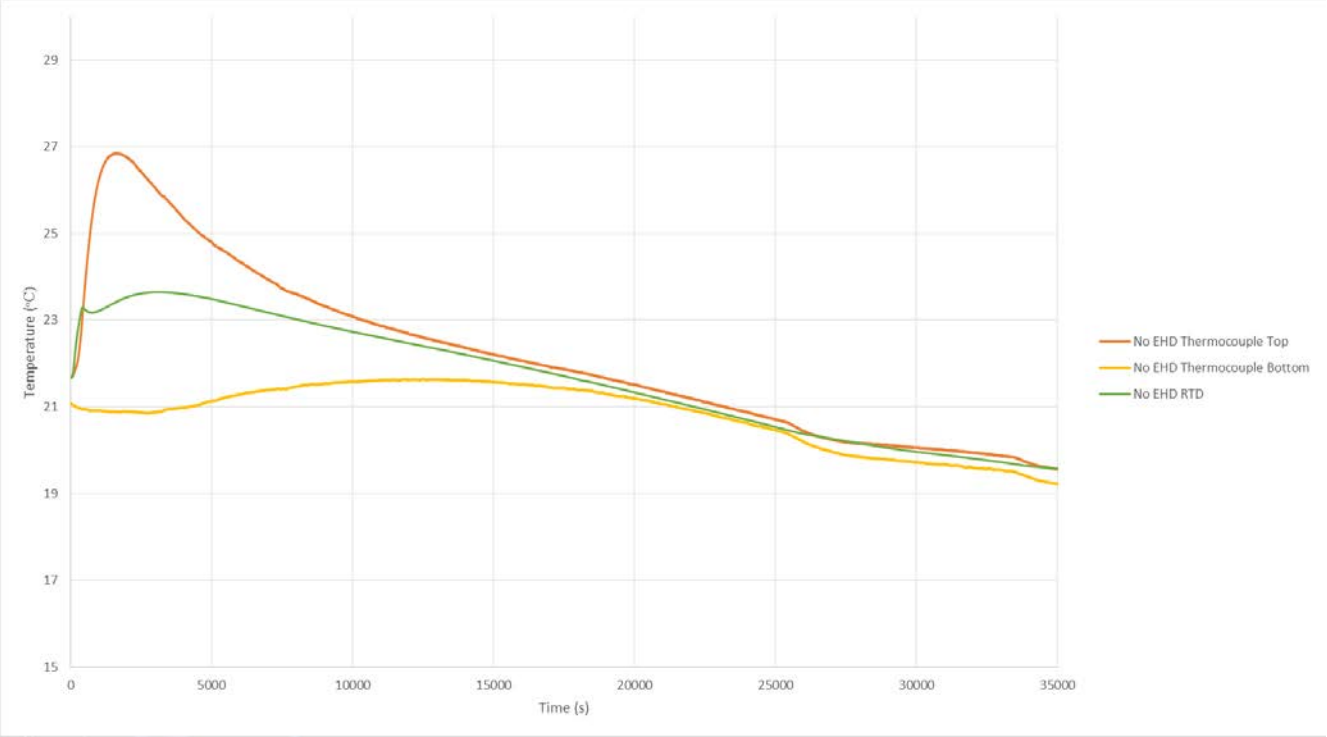

Figure 17: Temperature Data from Top Half, Center, and Bottom Half without EHD

Moving on, the data collected when the RTD was located in the center of the tank and the EHD electrode was supplied with 9,000 V produced some significant results. As seen in Figure 18, the heating of the tank started off the same as in Figure 18, however, this graph shows that immediately after the heater was turned off, and the EHD was turned on at 500 seconds, the temperature at the top and center of the tank both dropped over a full degree Celsius. The temperature at the bottom of the tank, which had no change in temperature while the heater was turned on, immediately began to rise once the EHD was started. The top thermocouple dropped to the same temperature as the bottom thermocouple when the EHD was turned on and followed the same temperature increase thereafter. The RTD which was located at the center of the tank was consistently higher than the thermocouples until all of the measuring devices peaked at about 24.5 ^{o}C. After that point, the temperatures were all the same, indicating that the tank had been fully mixed. This point occurred around 2,000 seconds, or at about 33 minutes. After 4,000 seconds the EHD was turned off and a small temperature gradient in the tank began to emerge once again.

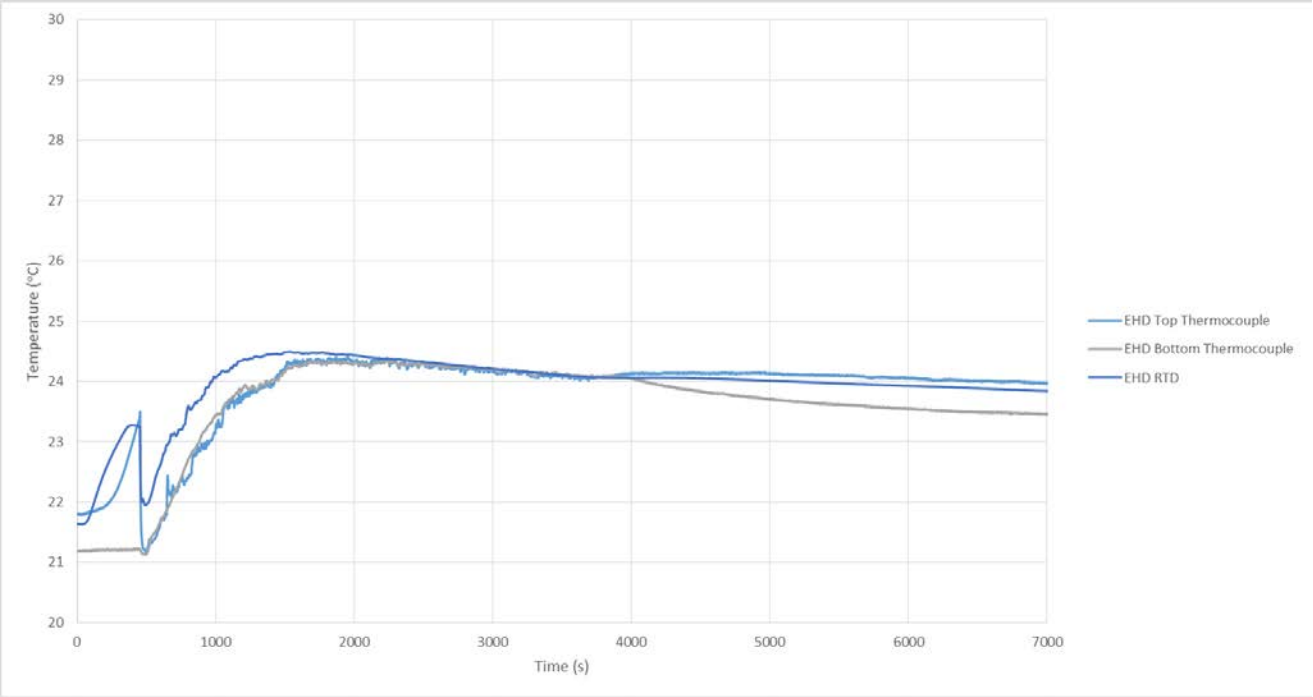

Figure 18: Temperature Data from Top Half, Center, and Bottom Half with EHD

The RTD was then moved to the top of the tank, and the thermocouples were left in their positions. Figure 19 shows the tank without EHD while Figure 20 shows the tank with EHD. As the tank was heated, the temperature at the very top of the tank measured by the RTD rose dramatically. The temperature rose 47 ^{o}C due to the fact that this area was so close to the heater. The temperatures of the thermocouples followed the same pattern as in the previous trials, which is to be expected if the trials were run properly. As shown in Figure 19 after the heater was turned off, the temperature at the top of the tank decreased exponentially. The temperature at the top thermocouple decreased slowly and eventually both temperatures at the top of the tank were about the same. This happened just after 5,000 seconds. The temperature at the bottom of the tank had almost no change the entire experiment. Eventually, after about 20,000 seconds, all three temperatures had reached their initial values. When 9,000 V were supplied to the EHD electrode, the cooling process was much different. The slope of the RTD's temperature was more

abrupt with EHD and trailed off more erratically as it got close to the temperature of the top thermocouple. As in the first tests, the temperature at the top thermocouple dropped down to match the bottom thermocouple and then they both began to rise simultaneously. At about 2,750 seconds, or 45 minutes, the temperatures were all within 0.1 ^{o}C of each other indicating the tank was fully mixed.

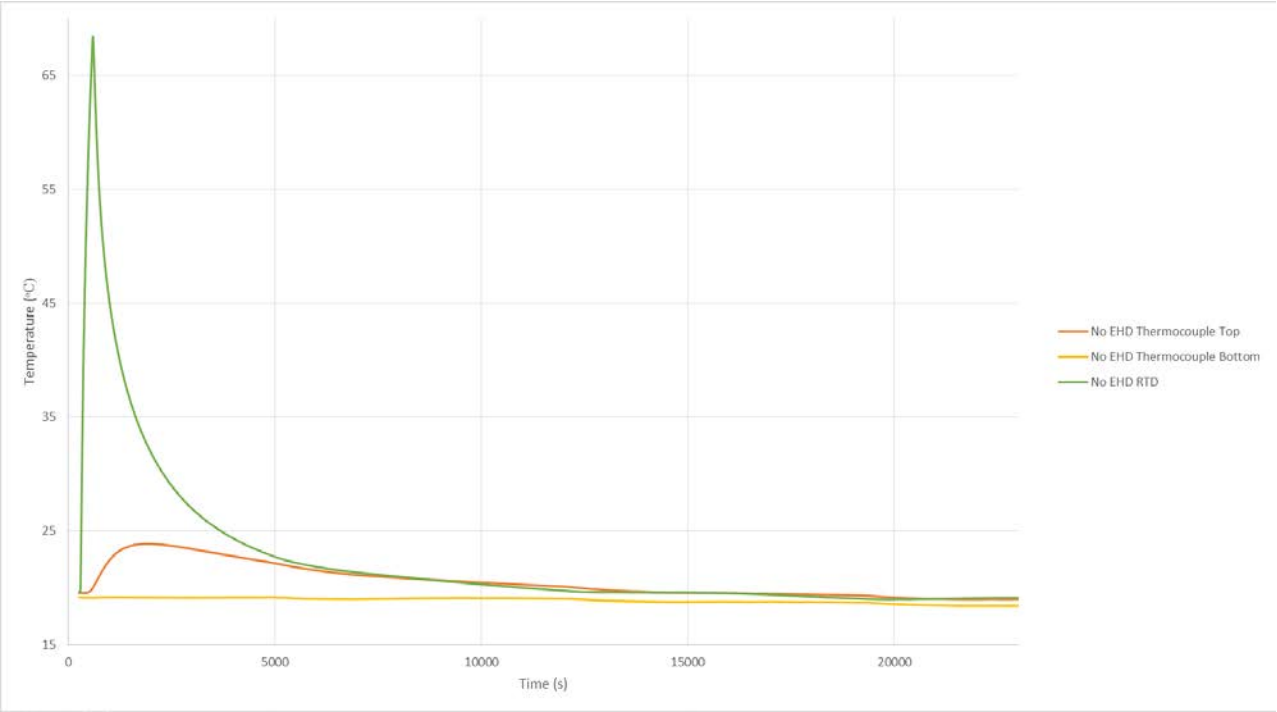

Figure 19: Temperature Data From Top Half, Top Inner Surface, and Bottom Half without EHD

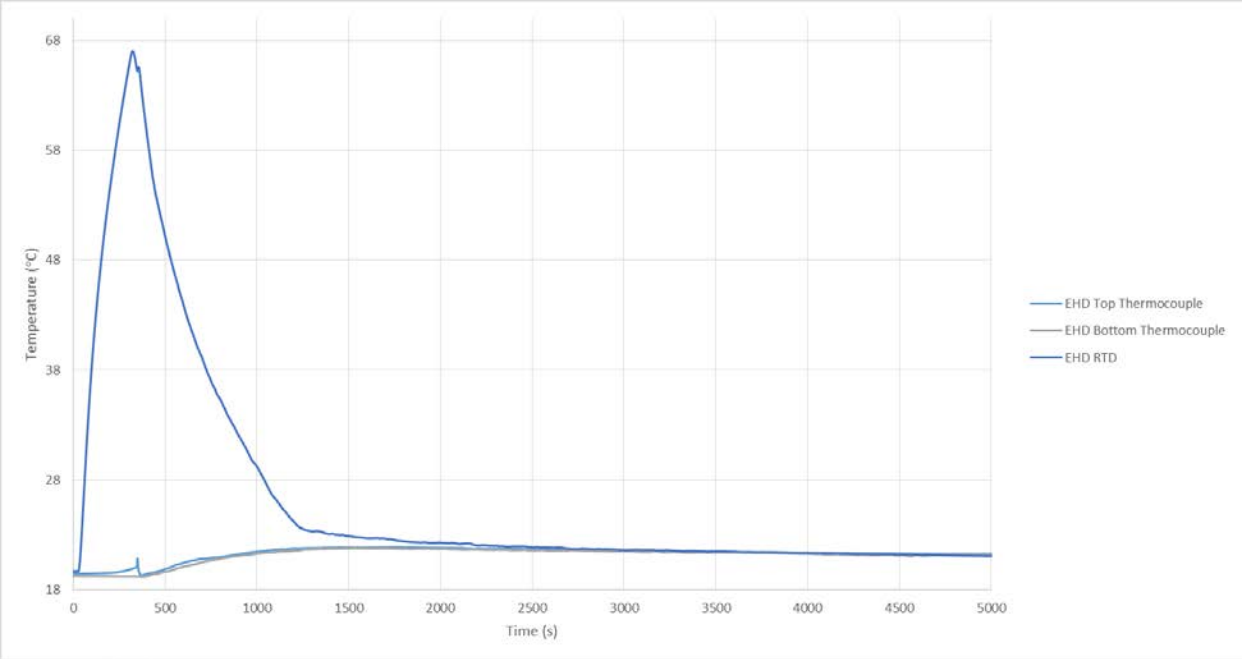

Figure 20: Temperature Data From Top Half, Top Inner Surface, and Bottom Half with EHD

4.2.2| Individual Comparisons

Next, the individual measurement device readings in the tank will be looked at more closely, comparing the results shown with and without EHD. The graph that is displayed in Figure 21 is the top thermocouple readings. This graph is able to display the effects of the EHD much more effectively than the previous graphs. The blue line displays the change in temperature measured when the EHD high voltage is turned on. From observing the graph, it can easily be seen that the EHD was turned on around the 500 seconds mark. At this point, the temperature drops rapidly before it starts to increase again before leveling off at around the 1,500 seconds mark. With the EHD on, the top thermocouple only reaches a temperature slightly above 24 ^{o}C. Without EHD, the top thermocouple climbs to a temperature slightly below 27 ^{o}C before it begins to decrease. Another graph of this data, after the RTD is relocated, can be found in Appendix E. This graph displays extremely similar trends to the one displayed in Figure 21.

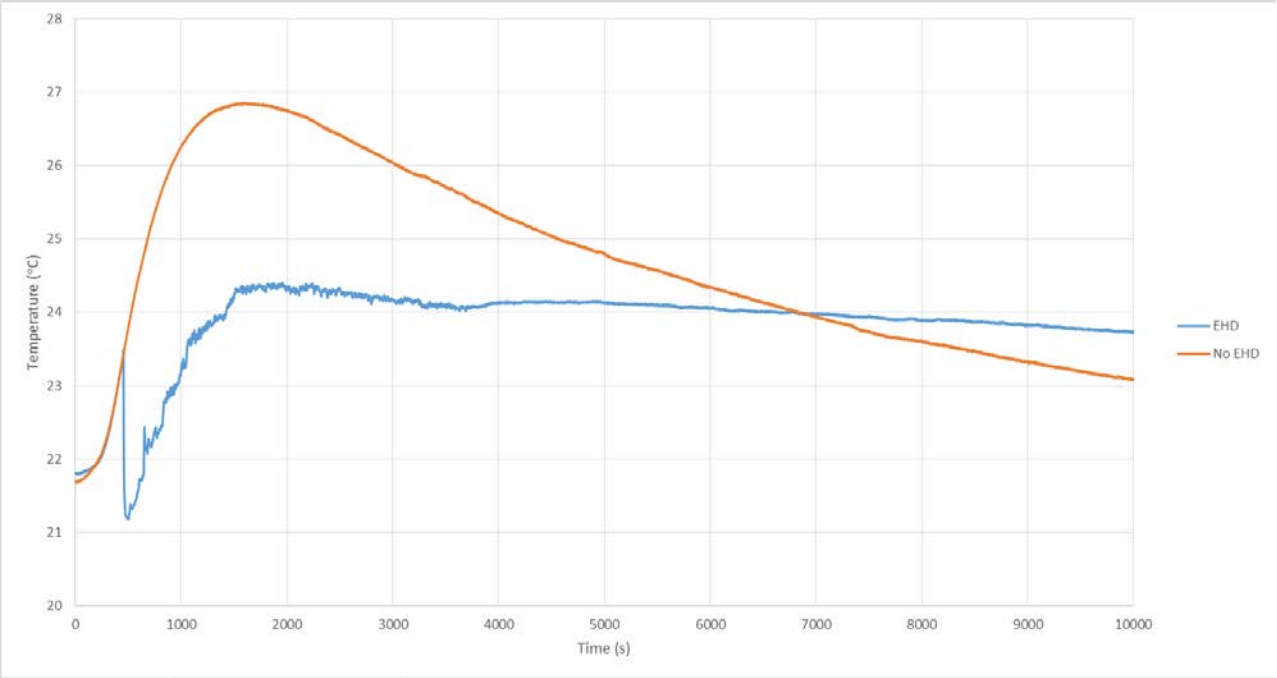

Figure 21: Comparison at Top Half with and without EHD

The next individual measurement device readings that are displayed are those of the bottom thermocouple in Figure 22. This graph also clearly displays that the EHD affects the working fluid within the tank. Again at around 500 seconds, the blue line displaying the EHD data shows that the temperature drops when the EHD voltage is turned on, but then increases rapidly to the same temperature as the top thermocouple at approximately 1,500 s. During this time in the experiment without EHD present, the bottom thermocouple remains almost fully unaffected until the around 4,000 seconds when natural convection reaches the bottom of the tank. As with the top thermocouple, shown in another graph of this data after the RTD is relocated, can be found in Appendix E. This graph displays very similar trends to the one displayed in Figure 22.

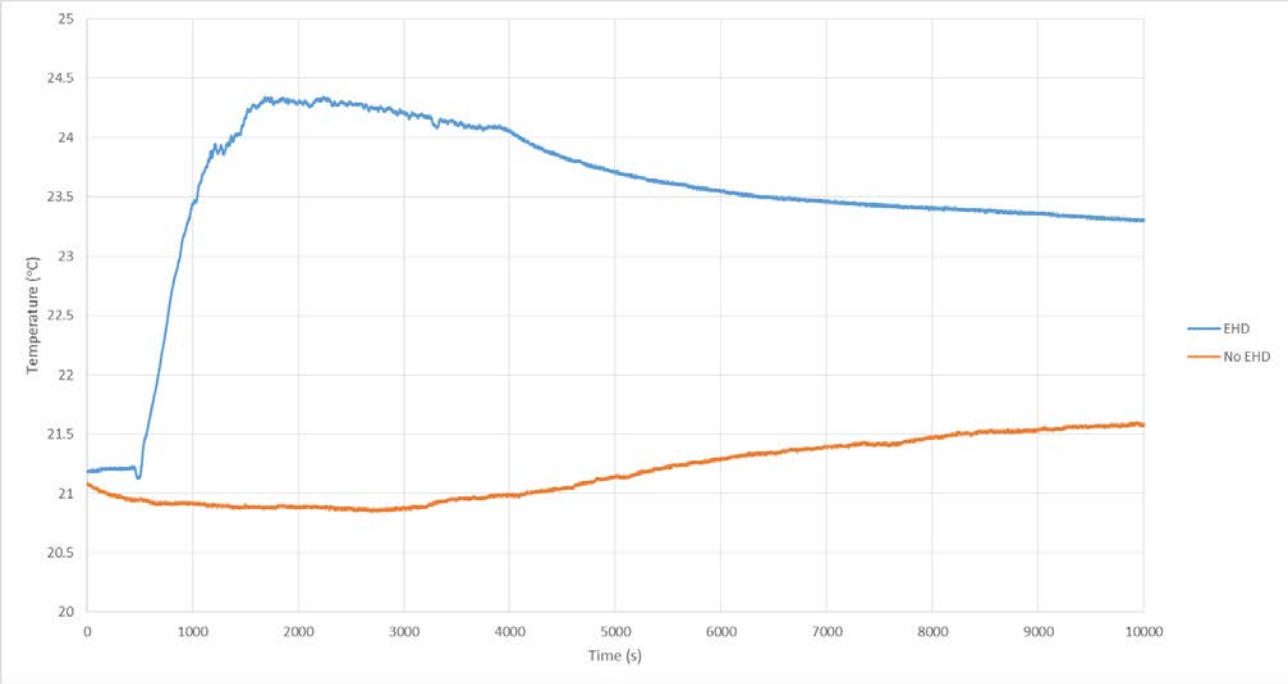

Figure 22: Comparison at Bottom Half with and without EHD

The RTD temperature readings when it is located in the exact center of the tank are displayed in Figure 23. This graph once again displays how the presence of EHD clearly causes mixing within the tank. As with the previous two graphs, at 500 seconds, when the EHD high voltage is turned on, the blue line displaying the EHD data immediately spikes downwards and then begins to progress upwards to slightly above 24 ^{o}C at 1,500 seconds where it becomes the same as both the thermocouples in the experiment. When there is no EHD, the temperature rises about 1.5 ^{o}C and then begins to regress back to where it started.

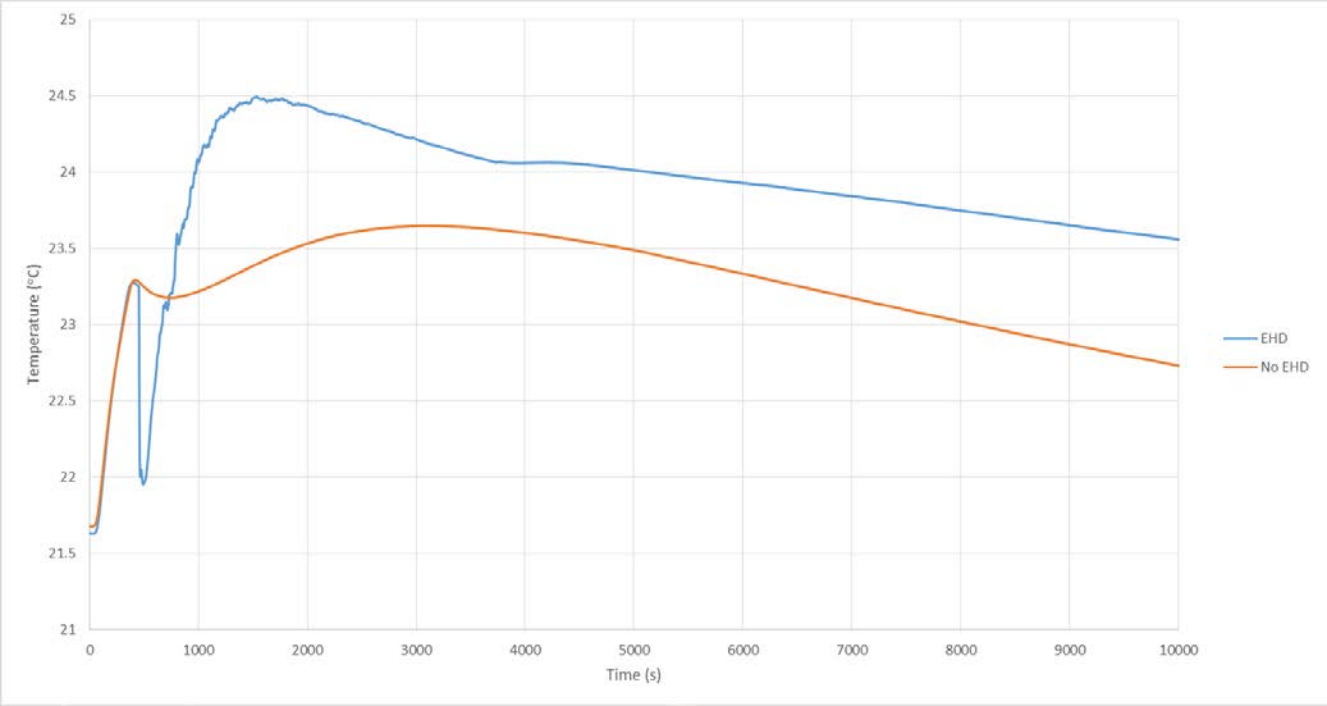

Figure 23: Comparison at Center with and without EHD

The last graph that is displayed in this results sections, shown in Figure 24, displays the behavior of the RTD after it is relocated 16 mm from the top of the tank. The temperature readings are significantly higher on this graph than any of the other individual measurement device graphs because the RTD is located very close to the heater during these trials. As seen in the graph, the temperature of the RTD quickly reaches approximately 68 ^{o}C right before the heater is turned off in both the EHD and no EHD trials. The difference between the two trials is that the temperature of the RTD in the EHD trial rapidly drops due to EHD mixing as compared to the slow decline in temperature of the no EHD trial.

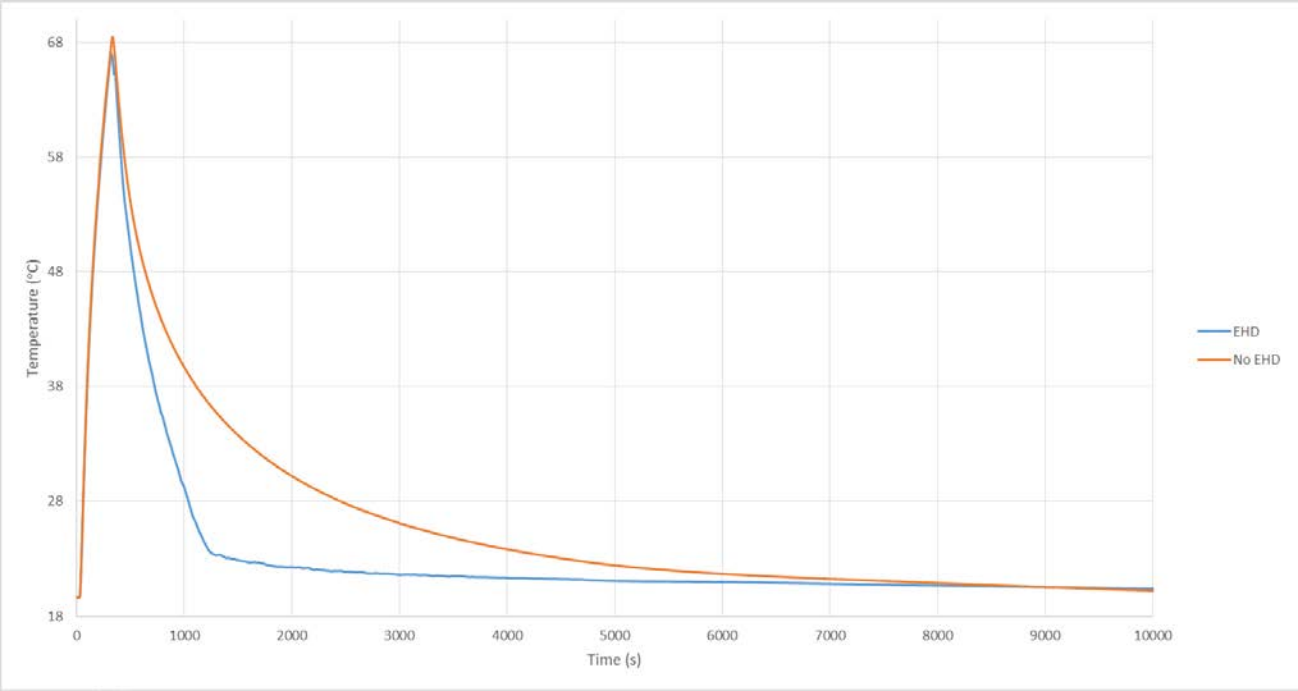

Figure 24: Comparison at Top Inner Surface with and without EHD

5 Impact

The topic of EHD conduction for mixing purposes is still very much unexplored. The research from this project has contributed to moving forward regarding existing knowledge of the subject. The project has shown a glimpse of the capabilities of the technology. There has been great promise shown for non-mechanical mixing using EHD conduction and this project has helped to prove that what before was only a theoretical concept and later a numerical model, actually works in real world settings. This opens up the door for more testing to be done and more knowledge to be gained. The data collected from this project will be directly used to develop numerical methods of analyzing EHD systems so that these systems can be improved upon.

The direction EHD technology is headed in is extremely impactful. As this technology grows, the possibilities for its uses expand and this project has contributed to that process. EHD mixed tanks have the potential to lead to zero boil off cryogenic tanks, which saves on costly fluid. Decreased costs due to no loss of fluid would make cryogenics a more accessible and efficient technology. As these tanks would be able to retain more fluid for longer amounts of time, it would allow for more fuel to be available for rockets and thus longer missions. Longer missions would lead to deeper space travel and potentially long distance manned missions.

Existing research, along with the research discussed in this report, could also lead to better electronic cooling devices for both terrestrial and zero gravity environments. This means that more efficient satellites could be made to stay in orbit longer, for example. The ability to precisely control EHD with an electric field will lead to smart technology which is already being tested on the International Space Station (ISS). As the technology develops, it can be used to help with cooling electrical components of the ISS as well as cooling specialized scientific

equipment on board for NASA. EHD is easily managed by controlling the electric fields produced through varying applied voltages and electrode configurations, which makes it very simple to use as a smart technology application. Enhanced cooling technology is not only important for space, but it is also extremely beneficial on earth. Cooling systems using EHD and dielectric fluids could be used to cool supercomputers and improve the processing power of these machines. Although the technology is not at this point now, the research done in this project is an important step in making an impact and looking to the future.

6 Ethical Considerations

Throughout the duration of research, experimentation, data collection, and analysis, it was imperative that ethical considerations be taken into account. As in many fields of research, ethical considerations are vital when conducting experimental research due to the fact that they are standards for acceptable practices. Furthermore, principles of ethics can play a large role in determining the validity and integrity of data and findings. Preliminary research was conducted to ensure there would be no copyright infringement when designing the apparatus. Experimental procedures were followed and safety precautions were adhered to allow for the safety of all researchers. The data provided was in no way fabricated or falsified. Detailed authorship accurately reflects the contributions of the respective individual and contributions have not been over evaluated or embellished. Prior to publication, limits of confidentiality were discussed with the faculty advisor.

7 Conclusions

In conclusion, the EHD mixing as theorized and represented with mechanical models proves to be viable through this experimentation. EHD conduction was proved to mix fluid in a tank through temperature measurements taken at various points throughout the tank. EHD allowed for the tank to reach a point of thermal equilibrium in 30-45 minutes. Without EHD it took over three hours to have a similar effect. The research value represented in this Major Qualifying Project is its investigation into the effects of electrohydrodynamic conduction mixing by two concentric electrodes within a storage tank. This study resulted in finding that the electrodes can generate enough voltage to effectively mix a fluid within the tank. In addition, this project further developed upon previous project efforts to apply the use of the electrohydrodynamic phenomena to an extraterrestrial cooling system. Lastly, this project provides a basis for further studies of EHD conduction mixing with the current experimental setup which will be able to test mixing at higher applied voltages with more suitable devices for velocity measurements. In conclusion, this experiment demonstrates EHD mixing as a positive alternative to current methods of mixing fluids within a storage tank.

References

[1] Adair, K., Alleyne, A., Barton, K., Ferreira, P., Georgiadis, J., Hardy, M., Kang, S., Lee, C., Mukhopdhyay, D., Park, J., Rogers, J., & Strano, M. (2007). High-resolution electrohydrodynamic jet printing. *Nature Materials,* 6, 782-789.

[2] Almeida, V., Culbertson, C., DePaoli, D., Jacobson, S., Ramsey, J., & Tsouris, C. (2003). Electrohydrodynamic mixing in microchannels. *AlChE Journal,* 49, 2181-2186.

[3] Barringer, S. & Gorty, A. (2011). Electrohydrodynamic Spraying of Chocolate. Jou*rnal of Food Processing and Preservation,* 35, 542-549.

[4] Bergstrom, T., Loiselle, J., Sears, A., & Tian, W. (2012). HAAS Machine WPI Quick Guide. Worcester Polytechnic Institute Haas Technical Education Center.

[5] Dancy, T., Kamat, O., Larkin, T., Seyed-Yagoobi, J., Talmor, M., & Yang, L. (2016). Flow distribution control in micro-scale via electrohydrodynamic conduction pumping. *IEEE Transactions on Industry Applications.*

[6] Davoodi, P., Jiang, J., Srinivasan, M., Wang, C., & Xie, J. (2015). Electrohydrodynamic atomization: A two-decade effort to produce and process micro-/nanoparticulate materials. *Chemical Engineering Science,* 125, 32-57.

[7] The Editors of Encyclopædia Britannica. (1998). Dielectric. *Encyclopædia Britannica, Inc.* Retrieved from https://www.britannica.com/science/dielectric

[8] The Editors of Encyclopædia Britannica (2006). Permittivity. *Encyclopædia Britannica, Inc.* Retrieved from https://www.britannica.com/science/permittivity

[9] Feng, Y., & Seyed-Yagoobi, J. (2004). Understanding of electrohydrodynamic conduction pumping phenomenon. *Physics of Fluids,* 16 (7), 2432-2441.

[10] Feng, Y., & Seyed-Yagoobi, J. (2006). Control of Liquid Flow Distribution Utilizing EHD Conduction Pumping Mechanism. *IEEE Transactions on Industry Applications*, 42 (2), 369-377.

[11] Friend, J. & Yeo, L. (2006). Electrohydrodynamic Flow for Microfluidic Mixing and Microparticle Manipulation. International Symposium on Electrohydrodynamics, 1-4.

[12] Fylladitakis, E., Moronism, A., & Theodoridis, M. (2014). Review on the History, Research, and Applications of Electrohydrodynamics. *IEEE Transactions on Plasma Science,* 42, 358-375.

[13] Jiang, C., Minchev, K., Seyed-Yagoobi, J., Shaw, B., Talmor, M., & Yang, L. (2015). Flow distribution control in meso scale via electrohydrodynamic conduction pumping. Proceedings of the *IEEE Industry Applications Society.*

[14] Mohapatra, S. (2006). An Overview of Liquid Coolants for Electronics Cooling. Electronics Cooling. Retrieved from https://www.electronics-cooling.com/2006/05/an-overview-of-liquid-coolants-for-electronics-cooling/

[15] NASA. (2016). STP-H5-Electro-Hydro Dynamics (STP-H5 EHD). Retrieved from https://www.nasa.gov/mission_pages/station/research/experiments/1993.html

[16] NASA. (2016). Zero Boil-Off Tank Experiment. Retrieved from https://issresearchproject.grc.nasa.gov/MSG/ZBOT/

[17] NASA. (2016). Zero Boil-Off Tank (ZBOT). Retrieved from https://www.nasa.gov/mission_pages/station/research/experiments/1270.html#results

[18] Patel, V., Robinson, F., & Seyed-Yagoobi, J. (2013). Terrestrial and Microgravity Experimental Study of Microscale Heat-Transport Device Driven by Electrohydrodynamic Conduction Pumping. *IEEE Transactions on Industry Applications,* 49, 2397-2401.

[19] Patel, V., Seyed-Yagoobi, J., Sinha-Ray, S., Sinha-Ray, S., & Yarin, A. (2016). Electrohydrodynamic Conduction Pumping-Driven Liquid Film Flow Boiling on Bare and Nanofiber-enhanced Surfaces. *ASME Journal of Heat Transfer,* 138.

[20] Pearson, M. & Seyed-Yagoobi, J. (2009). Advances in Electrohydrodynamic Conduction Pumping. *IEEE Transactions on Dielectrics and Electrical Insulation,* 16, 424-434.

[21] Seyed-Yagoobi, J. (2005). Electrohydrodynamic pumping of dielectric liquids. *Journal of Electrostatics,* 63, 861-869.

[22] Seyed-Yagoobi, J. & Yazdani, M. (2009). Fluid Circulation Within a Spherical Reservoir With EHD Conduction Pumping. *IEEE Transaction on Industry Applications,* 45, 1491-1498.

[23] Seyed-Yagoobi, J. & Yazdani, M. (2009). Thermal Homogenization in Spherical Reservoir by Electrohydrodynamic Phenomenon. *ASME Journal of Heat Transfer*, 131, 1-4.

Appendices

Appendix A: LabVIEW Block Diagram

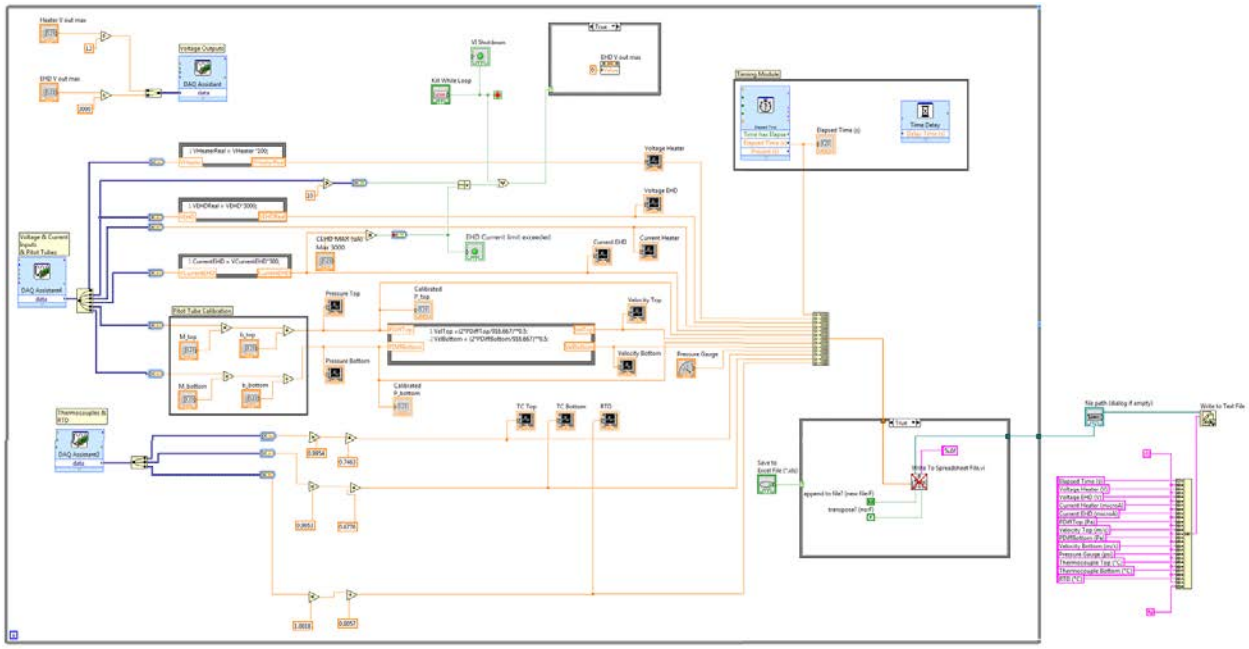

Appendix B: LabVIEW Front Panel

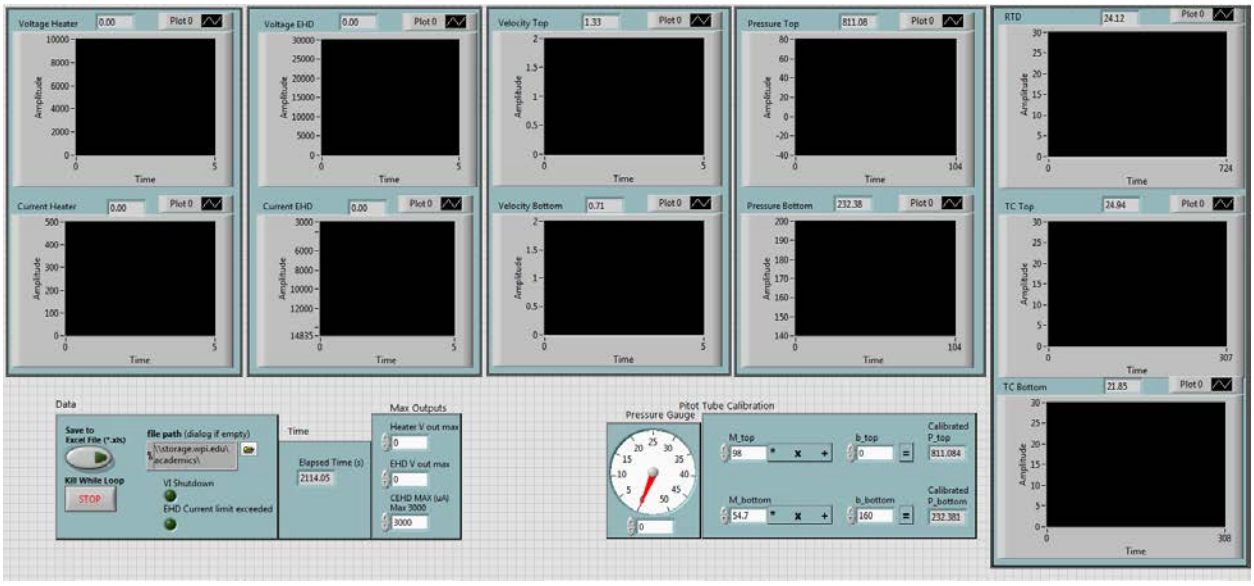

Appendix C: Differential Pressure Transducer Calibration

Top Differential Transducer Results		
Manometer Reading (in)	Voltage (V)	Pressure (Pa)
2.5	8.5	513.772
2	8.37	411.0176
1.5	7.99	308.2632
1	7.34	205.5088
0.5	6.28	102.7544
0.3	5.7	61.65264
0.2	5.4	41.10176
0.1	5.17	20.55088

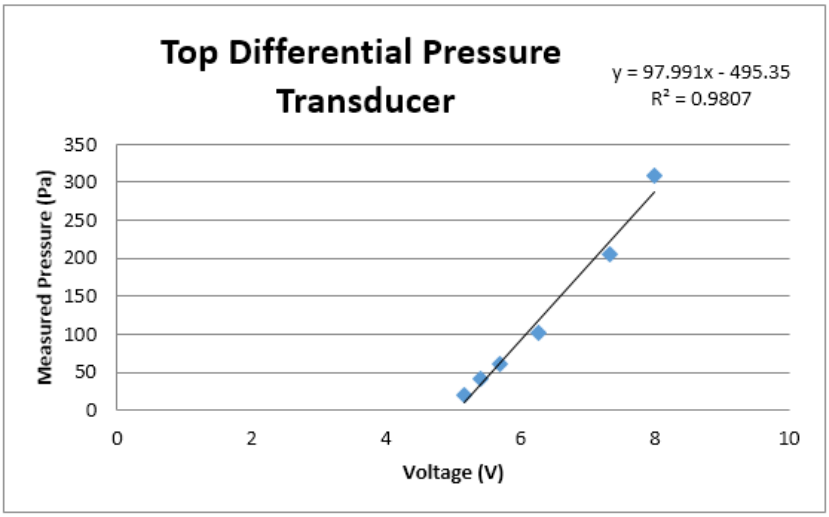

Bottom Differential Transducer Results		
Manometer Reading (in)	Voltage (V)	Pressure (Pa)
2.5	5.18	513.772
2	3.37	411.0176
1.5	1.71	308.2632
1	0.107	205.5088
0.5	-2	102.7544
0.3	-2.94	61.65264
0.2	-3.48	41.10176
0.1	-3.8	20.55088

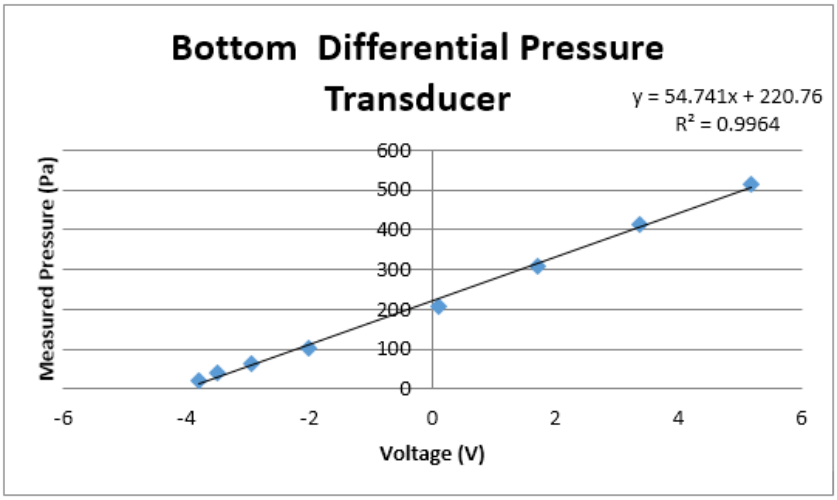
Bottom Differential Pressure Transducer
y = 54.741x + 220.76
R² = 0.9964
Measured Pressure (Pa)
600
500
400
300
200
100
0
-6
-4
-2
0
2
4
6
Voltage (V)

Appendix D: Heater Calculations

$pi := 3.1451926535897932384$

$v = \left(\frac{4}{3}\right)\cdot\left(\frac{11}{2}\right)^3 \frac{pi}{2} = 348.854$

$d := 0.93 \qquad Cp := 1.68$

$m := d \cdot v = 324.434$

$Td := 20$

$q := m \cdot Td \cdot Cp = 1.09 \times 10^4$

$Mv := 240 \qquad Mp := 400$

$R := \frac{Mv^2}{Mp} = 144$

v is volume (cm^3)
Cp is specific heat (kJ/kg*K)
Td is temperature difference (K)
m is mass (g)
q is heat (J)
Mp is maximum power (W)
Mv is maximum voltage (V)
R is resistance (ohms)
d is density of oil (g/cm^3)
P is heater power used in experiment (W)
Hf is heat flux (W/m^2)

To heat half the tank after 5 minutes the required voltage to apply is:

$\left(\sqrt{R \cdot \frac{q}{300}}\right) = 72.336$

Solving for heat flux from using 72 volts, with a current of 0.5 amps with the immersion heater:

$P := 72 \cdot .5 = 36$

The surface area of the immersion heater is 0.0828 m^2

$Hf := \frac{P}{0.828} = 43.478$

Appendix E: Thermocouple Results When RTD is Relocated